https://doi.org/10.1016/j.apenergy.2019.01.245

Title: A review of correlations and enhancement approaches for heat and mass transfer in liquid desiccant dehumidification system

Author: Tao Wen, Lin Lu*(vivien.lu@polyu.edu.hk)

Department of Building Services Engineering, The Hong Kong Polytechnic University, Hong Kong, China

Abstract: Liquid desiccant cooling systems are considered a promising technology for accurate humidity control and high energy efficiency. The dehumidifier and the regenerator are the two main components in the system, and their performance directly determines the system performance. This paper is a comprehensive review of the empirical correlations for the determination of mass transfer coefficient and moisture effectiveness in both adiabatic and internal cooling/heating dehumidifier/regenerators, and it further discusses approaches to enhance their mass transfer performance. These methods include structural improvements, such as structural modification, ultrasound atomisation and membrane-based modules, and modification of liquid desiccants, such as the addition of surfactants and nanoparticles. Finally, a brief summary and some suggestions for future work are outlined and addressed.

Key words: liquid desiccant cooling; mass transfer enhancement; structure modification; ultrasound atomisation; surfactant; nanofluid

Contents

Nomenclature			
A	Contact area (m^2)	Sc	Schmidt number ($\mu/\rho D$)
a	Surface area to volume ratio (m^2/m^3)	Sh	Sherwood number ($h_m d_e/\rho D$)
a_t	Total surface area (m^2/m^3)	T	Temperature (^oC)
a_w	Wetting surface area (m^2/m^3)	TEG	Triethylene glycol
CC	Cooling capacity (kJ/s)	V	volume of the device (m^3)
CCS	Constant curvature surface	Ve	Velocity (m/s)
CNT	Carbon nanotubes	VCS	Vapor compression system
c_0, c_1	Constants	w	Humidity content (g/kg)
d_e	Equivalent diameter (m)	We	Weber number ($G^2 d_e/\rho\sigma$)
d_m	Droplet dimeter (m)	X	Concentration (%)
D	Mass diffusion coefficient (m^2/s)	y	Mole fraction of water vapor (mol/mol)
f	Frequency (Hz)	y_a	Mole fraction of water vapor at bottom (mol/mol)
Fr	Froude number ($G^2/(\rho^2 g d_e)$)	y_b	Mole fraction of water vapor at top (mol/mol)
g	Gravitational acceleration (m/s^2)	Z	Packing height (m)
G	Mass flux ($kg/(m^2.s)$)	Greek symbols	
h	Enthalpy (kJ/kg)	ρ	Density (kg/m^3)
$HVAC$	Heating, ventilation, air-conditioning	μ	Dynamic viscosity (Pa.s)
h_m	Mass transfer coefficient ($kg/(m^2.s)$)	Δ	Change value
$h_{m,v}$	Volumetric mass transfer coefficient ($kg/(m^3.s)$)	η	Effectiveness
Le	Lewis number (α/D)	σ	Surface tension(N/m)
$LDCS$	Liquid desiccant cooling system	Subscripts	
$LiBr$	Lithium bromide	a	Air
$LiCl$	Lithium chloride	c	Critical
m	Mass flow rate (kg/s)	e	Equilibrium
$MARD$	Mean absolute relative devation	exp	Experimental value
$MWNTs$	Multi-walled carbon nanotubes	h	Enthalpy
M_s	Molecular weight (kg/mol)	i	Inlet
N	Number of data points	m	Moisture
Nu	Nusselt number (hd_e/λ)	n	Index

P	Pressure (Pa)	*o*	Outlet
PFHE	Plate-fin heat exchanger	*pre*	Predicted value
R	Gas constant (J/(mol.K))	*s*	Solution
Re	Reynolds number	*w*	Cooling water
		*	Equivalent value

1 Introduction

Statistics have shown that people nowadays spend 70%–90% of their lives inside buildings [1]. With the improvement of people's living standards, the high demand for thermal comfort in indoor environments has become urgent and strict. The main factors that affect thermal comfort are the body's gain and loss of heat, which are affected by factors such as metabolic rate, indoor temperature, relative humidity and air speed [2]. Among these influencing factors, the indoor temperature and humidity are often regarded as the two most important and controllable ones for a comfortable indoor environment [3, 4]. Nowadays, vapour compression cooling system (VCS) is used worldwide to deal with the sensible and latent load for buildings. Currently, urban buildings and infrastructure account for 33% of total energy consumption in the United States [5], 19.5% in China [6] and 40% in European countries [7], and these proportions are expected to increase in the foreseeable future, as shown in Fig. 1 [8]. The energy required by heating, ventilation and air-conditioning (HVAC) systems accounts for as much as 50% [9] of the abovementioned energy consumption. What makes the situation even worse is that traditional air-conditioning systems have long been criticised for their heavy dependence on electric energy and limited ability to control humidity [10-14]. In a VCS, the processed fresh air is first cooled to below the dew point temperature for dehumidification and then reheated before being delivered into the air-conditioned room, which is a waste of energy. To avoid the reheating process and improve the energy efficiency of the whole HVAC system, it has been suggested that the sensible and latent loads be dealt with separately [15, 16].

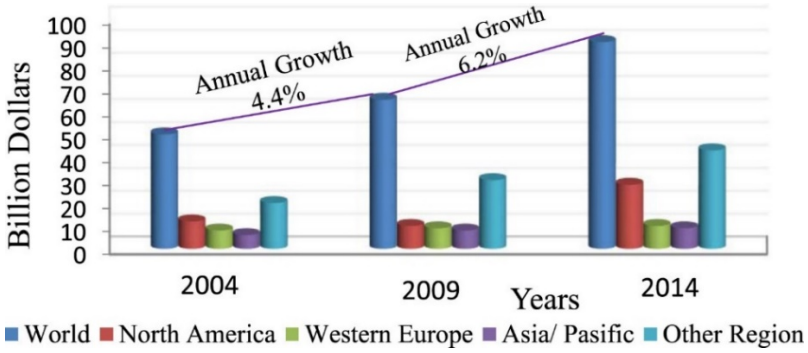

Fig. 1. HVAC equipment demand and annual growth [8].

The sensible load can be removed by a cooling coil; the latent load in the form of extra water vapour in the processed air can be dealt with using various approaches, such as electrochemical dehumidification, liquid desiccant dehumidification and solid desiccant dehumidification [17, 18]. Among these approaches, liquid desiccant dehumidification has drawn increasing attention in recent years because of its ability to accurately control humidity and its great energy-saving potential. Unlike VCS, which relies heavily on electric power consumption, liquid desiccant cooling system (LDCS) is able to use low-grade energy sources such as solar thermal energy, geothermal energy and waste heat in power stations [8, 19, 20], which helps to significantly improve the system energy efficiency. Compared with conventional VCSs, LDCS has the potential of energy conservation up to 30%–50% [21].

Because of their various merits and promising application prospects, LDCS becomes a research hotspot in recent decades. Many studies have focused on the thermal properties of liquid desiccants [22-24], the heat and mass transfer characteristics in dehumidifier/regenerators [10, 15, 25-28] and system energy efficiency analysis [29-32]. Some literature reviews related to LDCSs are summarised in Table 1.

Table. 1. Summary of literature reviews of LDCS.

Authors	Aims
Daou et al. [33] (2006)	The paper introduced the operation principles and related technological applications of LDCS. Their feasibility and energy- and cost-saving potential were underscored.
Mei and Dai [34] (2008)	The paper gave a detailed account of the general features of the major desiccant dehumidification techniques and configurations of LDCS. Experimental and analytical studies to optimise the system performance were summarised. Some new hybrid systems related to LDCS in other areas were introduced.
Cheng and Zhang [35] (2013)	The paper reviewed recent theoretical and experimental works on solar thermal regeneration method and solar electrodialysis regeneration method of LDCS.
Mohammad et al. [36] (2013)	The paper surveyed the recent studies and development activities in LDCS combined with evaporative cooling technologies.
Yin et al. [37] (2014)	The paper reviewed the heat and mass transfer models, performance evaluation and technologies development for dehumidifier/regenerator. Many detailed systems using solar energy and new applications of LDCS were also reported.
Luo et al. [38] (2014)	The paper provided an overview various mathematical models for modelling the simultaneous heat and mass transfer process in the liquid desiccant dehumidifier.
Buker and Riffat [39] (2015)	The paper reviewed solar-assisted liquid desiccant cooling and its various applications, combined with evaporative air conditioning under different climates.
Rafique et al. [40] (2016)	The paper presented different commercially available liquid desiccants and their composites. Different configurations of liquid desiccant dehumidifiers and their advantages and drawbacks were analysed.

Salam and Simonson [41] (2016)	The paper gave a comprehensive overview of LDCS equipment and systems and identified gaps in the literature to be considered by future research.
Gómez-Castro et al. [42] (2018)	The paper summarised theoretical and experimental studies on solar thermal regeneration methods of the hygroscopic solutions used in LDCS. The information about several configurations of regenerators and their performance were covered.
Fekadu and Subudhi [8] (2018)	The review showed the importance of renewable energy, thermal comfort and thermophysical properties of liquid desiccants, systematic design and scientific ways of using liquid desiccants in air conditioning for the future generation.

The literature reviews introduced various aspects of LDCS, such as liquid desiccant materials [40], experimental studies on thermal components of dehumidifiers and regenerators [35, 40, 41], mathematical models for dehumidifier/regenerators and systems [38] and regeneration models by renewable energy [8, 42]. Even though Yin et al. [37] simply summarised some empirical correlations for mass transfer efficiency, the summary was far from sufficient. Other reviews focused only on the research areas mentioned above and paid less attention to the determination of mass transfer performance in LDCS. Apparently, as two of the most important components in LDCS, the heat and mass transfer characteristics in dehumidifiers and regenerators play vital roles in the determination of component and system performance. When evaluating the heat and mass transfer performance in these two components, performance criteria such as mass transfer coefficient, dehumidification/regeneration rate and enthalpy effectiveness are adopted. For the convenience of engineering application, these performance criteria are often fitted as empirical correlations on the basis of experimental and theoretical analysis. Consequently, it is meaningful and necessary to collect these correlations and summarise their application ranges and conditions. Unfortunately, few studies have ever summarised these empirical correlations from previous investigations to guide dehumidifier/regenerator and LDCS design. Moreover, to improve the heat and mass transfer performance in dehumidifier/regenerators, relevant measures have been taken by scholars in various aspects. The literature reviews summarised in Table 1 did not pay enough attention to relevant heat and mass transfer enhancement methods in dehumidifier/regenerators, which are valuable for the improvement of component and system performance.

Unlike previous literature reviews on LDCS, this study aims to review the empirical correlations for the prediction of mass transfer performance and various approaches for enhancement of the heat and mass transfer performance in dehumidifier/regenerators for the first time. First, the operating principles and performance criteria of LDCS are briefly introduced, and some empirical correlations to calculate the mass transfer coefficient and effectiveness are then

summarised. Various methods to enhance the heat and mass transfer performance in dehumidifier/regenerators are discussed, and some suggestions for future study of LDCS are made.

2 Working principle and mass transfer criteria

2.1 Heat and mass transfer mechanism in dehumidifier/regenerators

A schematic diagram of an LDCS is illustrated in Fig. 2. A dehumidifier is used to absorb the extra water vapour from the processed air. A low-temperature, high-concentration liquid desiccant such as lithium chloride solution or lithium bromide solution is distributed from the top of the dehumidifier and comes into contact with the moist air. Driven by the vapour pressure difference between the desiccant and the processed air, water vapour in the moist air is absorbed by the liquid desiccant. After the dehumidification process, the humidity of the moist air decreases, and the air is pumped into a cooling coil. Finally, fresh air with the desired temperature and humidity is delivered into the air-conditioned room. Simultaneously, a weak solution in the dehumidifier is pumped into the regenerator. To obtain a positive vapour pressure difference between the solution and the air for regeneration, the solution must be heated to a relatively high temperature. The low-temperature weak solution first exchanges heat with a strong solution at high temperature in heat exchanger #2, as shown in Fig. 2. The solution is then heated in heat exchanger #1, whose power is supplied by a solar collector, before being delivered to the regenerator.

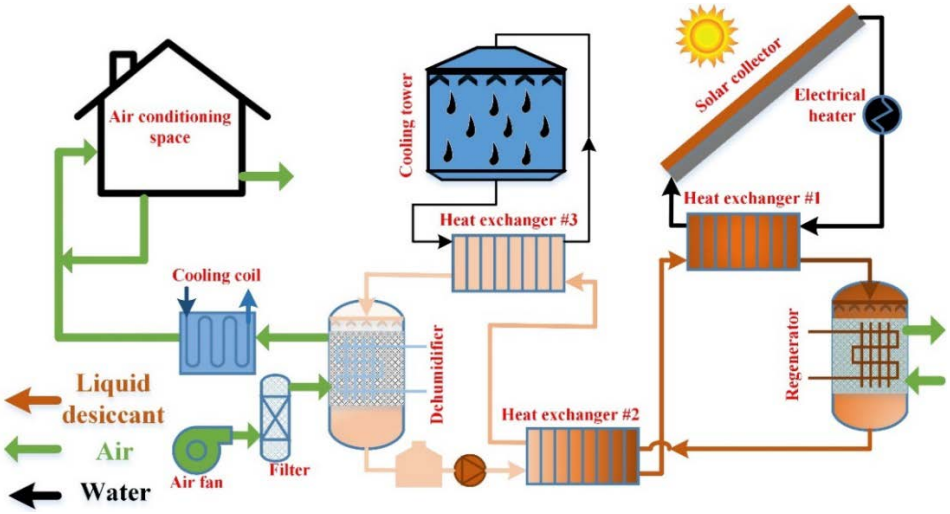

Fig. 2. Schematic diagram of an LDCS.

For a dehumidifier/regenerator, the spray type and packed-bed type shown in Fig. 3 were first adopted and studied [41]. However, because the spray type has the inherent drawbacks of low efficiency and a serious problem with liquid carryover, it was not a suitable candidate for LDCSs [43]. The two kinds of packing materials commonly used in packed beds are random and

structured packing. Compared with the packed bed filled with random packing, the one with structured packing has the advantages of high efficiency and high capacity of heat and mass transfer. It also has a smaller drop in air pressure drop during dehumidification/regeneration [44, 45]. Even though the packed-bed dehumidifier/regenerator is widely studied because of its simple configuration and large contact area between the air and the solution, some drawbacks greatly restrict their popularisation. First, the pressure drop on the air side is high when air flows through the packed column. Also, liquid carryover could occur under high air-flow rates, which is a great threat to indoor air quality. Moreover, during the dehumidification process, latent heat released by water vapour absorption is mainly absorbed by the liquid desiccant. As a result, the solution temperature gradually increases along the flow direction, which decreases the dehumidification performance. Similar problems are also expected to occur in adiabatic regenerators. To avoid the liquid carryover, a membrane-based dehumidifier/regenerator, illustrated in Fig. 4, was developed [46]. A permeable membrane with strong selectivity is used to totally separate the liquid desiccant and air during the dehumidification or regeneration process. To overcome the performance deterioration, an internal cooling/heating dehumidifier/regenerator was proposed, as shown in Fig. 5 [47]. Different from the packed-bed type that operates under adiabatic conditions, the internal cooling/heating type is cooled/heated during the dehumidification/regeneration process, which can greatly improve the heat and mass transfer performance [48, 49]. What's more, the pressure drop of the air can also be reduced, as well as the liquid carryover.

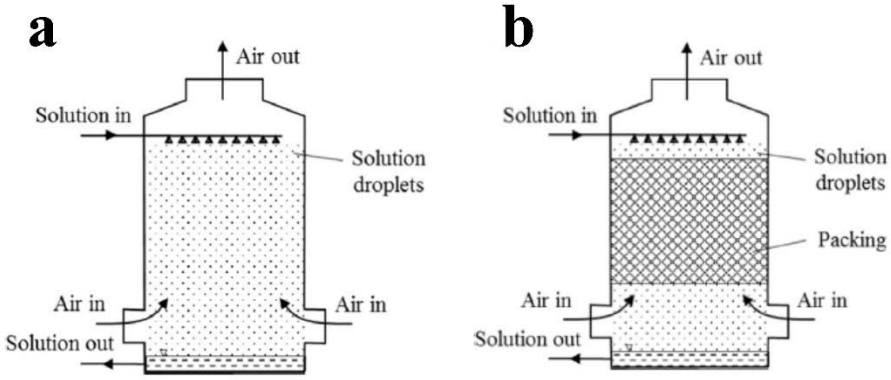

Fig. 3. Schematic diagram of (a) spray tower and (b) packed-bed dehumidifier/regenerator [41].

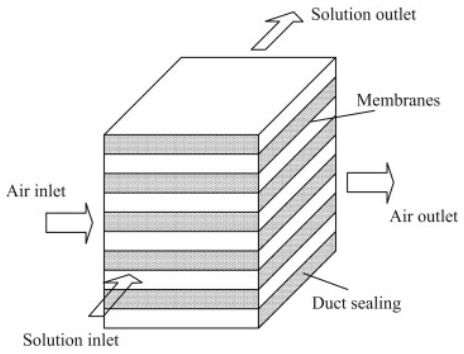

Fig. 4. Schematic diagram of a membrane-based dehumidifier/regenerator [46].

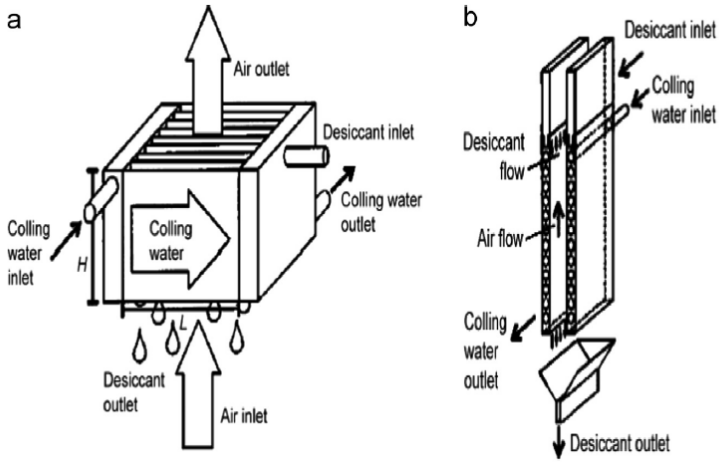

Fig. 5. Schematic diagram of an internal cooling falling-film dehumidifier [47].

2.2 Performance criteria

To evaluate the heat and mass transfer performance during dehumidification/regeneration, some criteria are introduced and summarised as follows:

(1) Absolute moisture removal Δw:

$$\Delta w = w_{a,i} - w_{a,o} \tag{1}$$

where w is the humidity content. The first subscript a stands for air. The subscripts i and o distinguish the inlet and outlet parameters, respectively. The absolute moisture removal is the humidity content difference between the inlet and outlet air.

(2) Moisture effectiveness η_m:

$$\eta_m = \frac{w_{a,i} - w_{a,o}}{w_{a,i} - w_e} \tag{2}$$

where w_e is the humidity content of the air under equilibrium with the inlet desiccant solution at its concentration and temperature. The moisture effectiveness represents the ratio between the actual absolute moisture removal and the potential greatest moisture removal.

(3) Moisture removal rate Δm:

$$\Delta m = m_a(w_{a,i} - w_{a,o}) \tag{3}$$

where m_a is the mass flow rate of the air. The moisture removal rate reflects the amount of moisture removed from the air per unit time.

(4) Enthalpy effectiveness η_h:

$$\eta_h = \frac{h_{a,i} - h_{a,o}}{h_{a,i} - h_e} \tag{4}$$

where h is the enthalpy and h_e stands for the equivalent enthalpy of the air under equilibrium with the inlet desiccant solution at its concentration and temperature.

(5) Mass transfer coefficient h_m [46]:

$$h_m = \frac{m_a}{A}\frac{w_{a,i} - w_{a,o}}{w_{a,i} - w_e} \tag{5}$$

where A is the contact area between the solution and the air. The heat transfer coefficient means the moisture absorption rate per unit area and time. Actually, the heat transfer coefficient h_m is often formulated as the dimensionless Sherwood number Sh:

$$Sh = \frac{h_m.d_e}{\rho_a.D_a} \tag{6}$$

where d_e is the equivalent diameter of the dehumidifier or regenerator. The terms ρ_a and D_a are the density and diffusion coefficient of air, respectively.

(6) Cooling capacity CC:

$$CC = m_a(h_{a,i} - h_{a,o}) \tag{7}$$

The cooling capacity means the enthalpy difference between the inlet and outlet air.

Among the abovementioned criteria, the moisture removal rate, moisture effectiveness, enthalpy effectiveness and mass transfer coefficient are the most common. They are widely used by researchers to evaluate the performance of various kinds of dehumidifier/regenerators. In addition to the aforementioned performance criteria, some other indices, such as latent heat ratio

[28], sensible heat ratio [41] and dehumidification perfection [50], have been adopted in some studies. It is noteworthy that only the mass transfer performance is considered in this review for several reasons. First, our research area focused on liquid desiccant dehumidification systems. In the LDCS, the mass transfer performance in terms of dehumidification and regeneration plays a more important role than heat transfer performance. Consequently, we only focus on the most important performance of the system. Compared with the research on mass transfer characteristics, the characteristics of heat transfer in various areas has drawn extensive attention. In other words, the research on heat transfer characteristics has been very thorough. As a result, we focus on mass transfer. Finally, only part of the mass transfer coefficient was given in the cited references. Therefore, to maintain the unity during description, we only considered mass transfer performance.

3 Empirical correlations for mass transfer coefficient and moisture effectiveness

When building a mathematical model for a dehumidifier/regenerator or designing a relevant mass transfer component in an LDCS, one of the most important issues is to determine the mass transfer behaviour between the solution and the air. Therefore, for the convenience of model development and engineering application, some empirical correlations to predict the mass transfer coefficient or humidity effectiveness have been proposed according to the corresponding experimental results. These correlations are summarised and introduced in this section.

3.1 Correlations for mass transfer coefficient

3.1.1 Adiabatic type

(1) Onda et al. correlation [51]

Early in 1968, Onda et al. [51] presented correlations on the mass transfer coefficients for gas absorption and desorption that were applicable for the vaporisation of water and gas absorption by organic solvents. Their formulations are expressed by the following Equation (8):

$$\begin{aligned} k_{m,a}\frac{RT_a}{a_t D_a} &= 5.23\left(\frac{G_a}{a_t\mu_a}\right)^{0.7}\left(\frac{\mu_a}{\rho_a D_a}\right)^{1/3}(a_t d_e)^{-2.0} \qquad \textit{air side} \\ k_{m,s}\left(\frac{\rho_s}{\mu_s g}\right)^{1/3} &= 0.0051\left(\frac{G_s}{a_w\mu_s}\right)^{0.7}\left(\frac{\mu_s}{\rho_s D_s}\right)^{1/3}(a_t d_e)^{-2.0} \quad \textit{solution side} \end{aligned} \tag{8}$$

The meanings of the parameters shown in Equation (8) can refer to the nomenclature. It is worth noting that the units of the mass transfer coefficient are $\mathrm{mol/(m^2.s)}$. The variables a_w and a_t are the wetting surface area and total surface area of packing, respectively, with units of $\mathrm{m^2/m^3}$. Their empirical relationship is expressed by Equation (9). The mass transfer coefficient of the air

side was applicable to the vaporisation process within ±30% error. The liquid-side mass transfer coefficient was applicable within ±20% error to the columns packed with Raschig rings, Berl saddles or spheres and rods and irrigated with organic solvents or water systems. The Onda et al. correlation has been widely used by subsequent researchers to predict the mass transfer coefficient in dehumidifier/regenerators [52-55].

$$\frac{a_w}{a_t} = 1 - \exp\{-1.45(\frac{\sigma_c}{\sigma_s})^{0.75} \mathrm{Re}_s^{0.1} Fr_s^{-0.05} We_s^{0.2}\} \tag{9}$$

(2) Chung et al. correlations [56]

Chung et al. [56] experimentally investigated the dehumidification performance of triethylene glycol (TEG) solution in random- and structure-packed beds. The materials were 5/8-in. polypropylene Flexi rings and 1/2-in. ceramic Intalox saddles for random packing and cross-corrugated cellulose and PVC for structured packing. Based on their experimental results, correlations to predict the mass transfer coefficient during dehumidification are listed in Equation (10).

$$\begin{aligned} k_m \frac{M_s d_e^2}{D_a \rho_a} &= 6.33\times10^{-5}(1-X_s)^{-0.09}\left(\frac{G_s}{G_a}\right)^{0.27} Sc_a^{0.333}\,\mathrm{Re}_a^{1.38} \quad \textit{Random packing} \\ k_m \frac{M_s d_e^2}{D_a \rho_a} &= 9.03\times10^{-6}(1-X_s)^{-0.05}\left(\frac{G_s}{G_a}\right)^{0.26} Sc_a^{0.333}\,\mathrm{Re}_a^{1.34} \quad \textit{Structured packing} \end{aligned} \tag{10}$$

The mass transfer coefficients under various conditions predicted by Equation (10) were within ±10% of the experimental data.

(3) Chung et al. correlation [45]

Chung et al. [45, 57] carried out extensive experiments to compare the dehumidification performance of lithium chloride (LiCl) solution in both random- and structure-packed beds. Cross-corrugated cellulose and polyvinyl chloride (PVC) were used as the structured packing, and polypropylene Flexi rings and ceramic Berl saddles were used as the random packing. Correlations for overall mass transfer coefficient, as shown in Equation (11), were proposed according to the experimental results.

$$
\begin{aligned}
k_m \frac{M_s d_e^2}{D_a \rho_a} &= 1.326\times10^{-4}(1-X_s)^{-0.94}\left(\frac{G_s}{G_a}\right)^{0.27} Sc_a^{0.333}\,\mathrm{Re}_a^{1.16} \quad \textit{Random packing} \\
k_m \frac{M_s d_e^2}{D_a \rho_a} &= 2.25\times10^{-4}(1-X_s)^{-0.75}\left(\frac{G_s}{G_a}\right)^{0.10} Sc_a^{0.333}\,\mathrm{Re}_a \qquad \textit{Structured packing}
\end{aligned}
\tag{11}
$$

As one can see, the form of Equation (11) for the LiCl solution is very similar to that of Equation (10) for the TEG solution. The differences between the experimental mass transfer coefficient and the predicted values were within $\pm 10\%$. Moreover, Koronaki et al. [58] adopted the correlation in their developed model to analyse the dehumidification performance of various liquid desiccants in a counter-flow adiabatic dehumidifier. Good agreement was found between the experimental data and the theoretical model in terms of air outlet temperature, air outlet humidity ratio and solution outlet temperature.

(4) Al-Farayedhi et al. correlation [59]

Al-Farayedhi et al. [59] conducted a theoretical study to deduce the mass transfer coefficient for an air–desiccant contact system with three liquid desiccants in a gauze-type structure-packed bed. The liquid desiccants were calcium chloride, lithium chloride and a mixture of 50% calcium chloride and 50% lithium chloride. The formulas for these correlations are shown in Equation (12).

$$
\begin{aligned}
k_{m,a} &= 0.55 V_{e,s}^{0.1} V_{e,a}^{0.79} \exp(-0.0293 T_a) \\
k_{m,s} &= 6.27 V_{e,s}^{0.4} V_{e,a}^{0.07} \exp(-0.033 T_s + 0.0066 X_s) \quad CaCl_2 \\
k_{m,s} &= 8.2 V_{e,s}^{0.4} V_{e,a}^{0.07} \exp(-0.038 T_s + 0.009 X_s) \quad LiCl \\
k_{m,s} &= 7.0 V_{e,s}^{0.4} V_{e,a}^{0.07} \exp(-0.0352 T_s + 0.0076 X_s) \quad Mixed
\end{aligned}
\tag{12}
$$

(5) Elsarrag et al. correlation [60]

Elsarrag et al. [60] carried out experiments to evaluate the dehumidification performance of a TEG solution in a packed bed filled with cross-corrugated cellulose-structured packing. Based on their experimental data and the data from Chung et al. [45], correlations to predict the mass transfer coefficient were developed as follows:

$$
\begin{aligned}
k_m \frac{M_s d_e^2}{D_a \rho_a} &= 6.18\times10^{-6}\left(1-\frac{P_s}{P_w}\right)^{-0.77}\left(\frac{G_s}{G_a}\right)^{0.55} Sc_a^{0.333}\,\mathrm{Re}^{1.3} \quad 0.88 < \frac{G_s}{G_a} < 2 \\
k_m \frac{M_s d_e^2}{D_a \rho_a} &= 0.52\left(1-\frac{P_s}{P_w}\right)^{-0.48}\left(\frac{G_s}{G_a}\right)^{0.55} Sc_a^{0.333}\,\mathrm{Re}^{0.2} \qquad 2 < \frac{G_s}{G_a} < 11
\end{aligned}
\tag{13}
$$

These correlations predicted the mass transfer coefficient values within ±15% of the experimental data.

It is noteworthy that in Equations (8) and (10)–(13), k_m represents the mass transfer coefficient with the units of $\mathrm{mol/(m^2.s)}$. Accordingly, its definition is also different from that given in Equation (5). It is defined as follows [45]:

$$k_m = \frac{M_v}{Z}\int_{y_a}^{y_b}\frac{(1-y)^*}{1-y}\frac{dy}{y-y^*} \tag{14}$$

The meaning of the symbols in Equation (14) can refer to the nomenclature. Because there is an integration in the equation, it is very difficult to determine the actual mass transfer coefficient. Chung et al. [45] calculated the mass transfer coefficient numerically by using the Simpson's integration method. Because determining this kind of mass transfer is very difficult during practical application, most subsequent investigators chose to employ the definition shown in Equation (5). Therefore, unless special explanation is given, the definition of mass transfer coefficient used herein is the one shown in Equation (5).

(6) Liu et al. correlation [61]

Liu et al. [61] experimentally identified the heat and mass transfer characteristics of the cross-flow packed-bed dehumidifier/regenerator using a LiBr solution. They adopted the Celdek structured packing material, which is made of corrugated cellulose paper with different flute angles. The developed correlations were based on the correlation developed by Chung and Wu [62] and are listed in Equation (15).

$$\begin{aligned} Sh_a &= 0.0011(1-X_s)^{1.913}\left(\frac{G_s}{G_a}\right)^{0.396} Sc_a^{0.333}\,\mathrm{Re}_a^{1.363} \qquad \textit{Dehumidification} \\ Sh_a &= 5.59\times10^{-6}(1-X_s)^{-5.353}\left(\frac{G_s}{G_a}\right)^{0.617} Sc_a^{0.333}\,\mathrm{Re}_a^{1.546} \qquad \textit{Regeneration} \end{aligned} \tag{15}$$

By adopting Equation (15), the enthalpy and humidity effectiveness was calculated with average absolute discrepancies of 7.9% and 8.5%, respectively, for dehumidification and 5.8% and 6.9%, respectively, for regeneration.

(7) Zhang et al. correlation [63]

Zhang et al. [63] evaluated the overall mass transfer performance of a structured packing dehumidifier/regenerator using a LiCl solution. The cross-flow configuration between the air and

the liquid desiccant was arranged in their experiments. According to the test results, correlations to predict the mass transfer coefficients were developed, as shown in Equation (16).

$$\begin{aligned} h_m \frac{d_e}{D_a \rho_a} &= 0.0038 Sc_a^{0.33} \mathrm{Re}_a^{0.52} Sc_s^{0.33} \mathrm{Re}_s^{0.28} \qquad \textit{Dehumidification} \\ h_m \frac{d_e}{D_a \rho_a} &= 0.0038 Sc_a^{0.33} \mathrm{Re}_a^{0.38} Sc_s^{0.33} \mathrm{Re}_s^{0.39} \qquad \textit{Regeneration} \end{aligned} \tag{16}$$

The deviations between the experimental findings and the predicted ones were approximately $\pm 20\%$.

(8) Langroudi et al. correlation [64]

Langroudi et al. [64] proposed a correlation for the calculation of a *Sh* number for a random packed dehumidifier. The packing material was glass beads, and the liquid desiccant was a LiBr solution. Counter-flow was arranged in the dehumidifier during experiment. The correlation is presented in Equation (17).

$$Sh_a = 0.158(1 - X_s)^{1.102} \left(\frac{m_s}{m_a} \right)^{0.115} Sc_a^{0.333} \mathrm{Re}_a^{0.689} \tag{17}$$

The absolute average deviation between the measured *Sh* numbers and the calculated ones was 2.14%, with most of the discrepancies within $\pm 9\%$.

(9) Su et al. correlation [65]

Su et al. [65] recently developed an empirical correlation for a cross-flow dehumidifier with structured packing in a frost-free heat pump system under cold winter operating conditions. The LiCl solution was chosen as the liquid desiccant. Based on their experimental results, the correlation for mass transfer coefficient was fitted as follows:

$$h_m = 2.2596 X_s^{-0.5818} G_s^{-0.31952} G_a^{1.1019} \tag{18}$$

The results indicated that the absolute discrepancies between the experimental mass transfer coefficient and predicted ones were within 20%, and the average error was 5.4%.

(10) Varela et al. correlation [66]

Based on the experimental data obtained from an adiabatic dehumidifier made of a structure-packed bed, Varela et al. [66] also proposed a correlation. Crossflow between a LiCl solution and the processed air was arranged in the dehumidifier/regenerator. By nonlinear regression analysis, the following correlations for mass transfer coefficient during dehumidification and regeneration were obtained:

$$h_m \frac{d_e}{D_a \rho_a} = 0.0307\,\mathrm{Re}_a^{0.5519}\,\mathrm{Re}_s^{0.2833} \qquad \textit{Dehumidification}$$
$$h_m \frac{d_e}{D_a \rho_a} = 0.0109\,\mathrm{Re}_a^{0.4642}\,\mathrm{Re}_s^{0.4818} \qquad \textit{Regeneration} \tag{19}$$

It was found that deviations between the measured mass transfer coefficients and the calculated ones were mostly within the error band of $\pm 10\%$.

Detailed information for the above summarised correlations for mass transfer characteristics is given in Table 2.

Table. 2. Summary of mass transfer coefficient correlations for adiabatic type.

Authors	Mode[a]	Flow pattern[b]	Desic-cant	Conditions[c]	Accuracy
Onda et al. [51]	D, R	R			±30%
Chung et al. [56]	D	Co, S, R	TEG	m_a :0.008-0.032; T_a :22.7-28.4; w_a :9.6-18 m_s :0.11-0.23; T_s :16.2-23.2; X_s :90-95	±10%
Chung et al. [45]	D	Co, S, R	LiCl	m_a :0.015-0.032; T_a :20.4-29.6; w_a :10-17.8 m_s :0.11-0.23; T_s :16.5-21; X_s :30-38	±10%
Al-Farayedhi et al. [60]	D	S	$CaCl_2$, LiCl, mixed	$V_{a,e}$:8.5-14.5; T_a :30-70; $V_{s,e}$:0.03-0.27; T_s :30-60; X_s :35-45($CaCl_2$), 30-40(LiCl)	
Elsarrag et al. [60]	D	Co, S	TEG	G_a :0.94-2.2; G_s :1.75-2.2	±15%
Liu et al. [61]	D, R	Cr, S	LiBr	G_a :1.58-2.5; T_a :24.7-35.4; w_a :9.5-21 G_s :2.04-5.35; T_s :19.7-29.5; X_s :42.2-54.8	≤ 9%
Zhang et al. [63]	D, R	Cr, S	LiCl	T_a :0-50; w_a :1.5-21; T_s :060; X_s :30-40	±20%
Langroudi et al. [64]	D	Co, R	LiBr	V_a :2.5-4.5; T_a :25-40; w_a :11.8-20 m_s :0.012-0.14; T_s :20-30; X_s :38-50	±9%
Su et al. [65]	D	Cr, S	LiCl	G_a :1.89-4.4; T_a :0.1-5.2; w_a :2.4-3.6 G_s :1.45-4.22; T_s :-4.2-1.1; X_s :23.6-35	±20%
Varela et al. [66]	D, R	Cr, S	LiCl	V_a :0.41-2.38; T_a :34; w_a :19.4-19.64 m_s :0.04-0.2; T_s :17,50; X_s :29.18-30.15	±10%

a: D: dehumidification; R: regeneration;

b: Co: counter-flow; Cr: cross-flow; S: structured packing; R: random packing;

c: G_a , G_s (kg/m^2.s); m_a , m_s (kg/s); T_a , T_s (°C); $V_{a,e}$, $V_{s,e}$, V_a (m/s); w_a (g/kg); X_s (%)

Generally, it is better to evaluate the prediction accuracy of the empirical correlation with existing experimental data. Consequently, we tried to collect experimental data from previous studies. Some examples are summarised in Table 3.

Table. 3. Summary of mass transfer coefficient data for adiabatic type.

Authors	Mode[a]	Flow pattern[b]	Solution	Remarks
Liu et al. [61]	D, R	Cr, S	LiBr	Experimental data were not given in detail.
Zhang et al. [63]	D, R	Cr, S	LiCl	Usable.
Langroudi et al. [64]	D	Co, R	LiBr	Equivalent diameter was not indicated, and some experimental conditions were not given.
Su et al. [65]	D	Cr, S	LiCl	Equivalent diameter was not indicated.
Varela et al. [66]	D, R	Cr, S	LiCl	Equivalent diameter was not indicated, and the calculation of solution Reynolds number was unclear.
Bassuoni [67]	D, R	Cr, S	$CaCl_2$	Equivalent diameter was not indicated.
Chen et al. [68]	D, R	Cr, S	LiCl	Equivalent diameter was not indicated, and some experimental conditions were not given.
Huang et al. [69]	R	Cr, S	EG	Equivalent diameter was not indicated, and some experimental conditions were not given.

a: D: dehumidification; R: regeneration;
b: Co: counter-flow; Cr: cross-flow; S: structured packing; R: random packing;

Unfortunately, little of the experimental data shown in Table 3 could be used for evaluation owing to the lack of equivalent diameter and indispensable operating conditions. The same situation also applied in other previous publications. Instead, we compared the predication results of various correlations under the operating conditions shown in Table 4. It is noteworthy that the conditions shown in Table 4 were roughly determined according to the data sources shown in Table 3 and a review paper by Jain and Bansal [54]. Only the correlations of Liu et al. [61], Langoudi et al. [64], Zhang et al. [63], Su et al. [65] and Varela et al. [66] were compared because their form of mass transfer coefficient was easy to determine in practical application. The other correlations presented in the manuscripts, such as those of Onda et al. [51] and Chuang et al. [56], were not included in the evaluation because the definition of the mass transfer coefficient for these equations contained an integration, as shown in Equation (14). In practical application, it is very difficult to determine the actual mass transfer coefficient. The dehumidifier was assumed to be cubic (Length × Width × Height = 0.5 × 0.5 × 0.5 m) with an equivalent diameter of 0.01 m. The comparison results are shown in the form of the *Sh* number in Fig. 6.

Table. 4. Operating conditions of different parameters.

Parameter	T_a (°C)	m_a (kg/s)	T_s (°C)	m_s (kg/s)	X_s (%)
Value	25-39	0.2-1.6	15-36	0.5-4.0	30-54

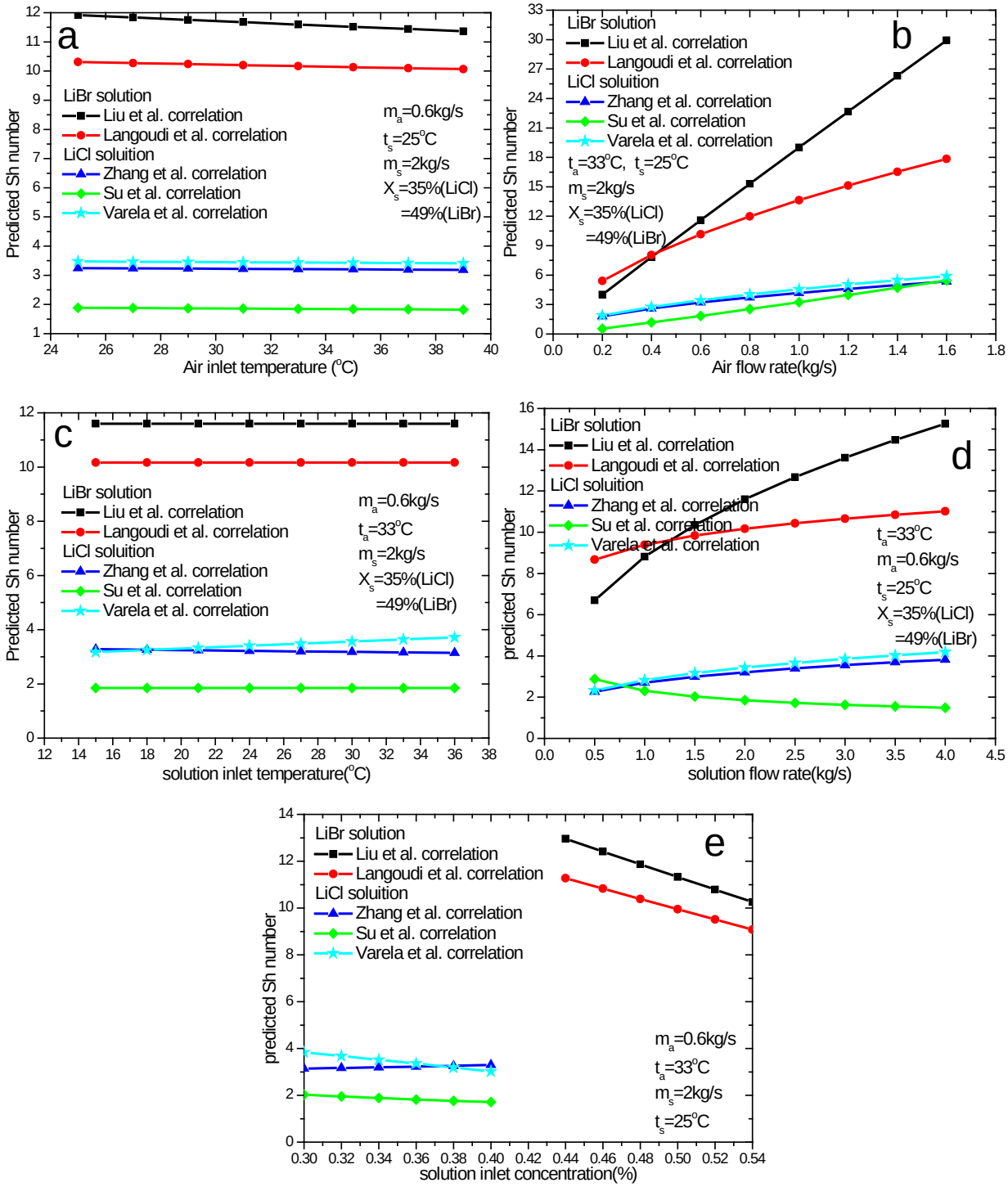

Fig. 6. Comparison of *Sh* number between different correlations for adiabatic dehumidifier.

Because the correlations of Liu et al. [61] and Langoudi et al. [64] are applicable for a LiBr solution, the concentration was set to be 44%–54%, which differed from that for the LiCl solution (30%–40%). Such attempts were intended to make the comparison comparable under similar mass transfer driving forces. According to Fig. 6, the changing trends of different correlations under

various operating conditions are similar. The correlations of Liu et al. [61] and Langoudi et al. [64] for LiBr solutions had comparable *Sh* numbers and were higher than the other three correlations for LiCl solutions. Similarly, the other three correlations of Zhang et al. [63], Su et al. [65] and Varela et al. [66] for LiCl solutions also shared similar *Sh* numbers under the same conditions.

3.1.2 Internal cooling/heating type

(1) Yin et al. correlation [70]

Yin et al. [70] advanced empirical correlations to calculate the Sherwood number during dehumidification/regeneration in an internal cooling/heating falling-film dehumidifier/regenerator based on their experimental results. LiCl solution was used as the liquid desiccant. The flow pattern was arranged to be parallel.

$$\begin{aligned} Sh_a &= 0.345 T_s^{-2.991} Sc_a^{0.33} \mathrm{Re}_a^{1.56} / \rho_a \qquad \textit{Dehumidification} \\ Sh_a &= 2.582\times10^{5} T_s^{-3.36} Sc_a^{0.33} \mathrm{Re}_a^{1.55} / \rho_a \qquad \textit{Regeneration} \end{aligned} \tag{20}$$

It is noteworthy that the term ρ_a in the denominator in Equation (20) was not involved in the original format developed by Yin et al. [70] owing to the special definition of mass transfer coefficient. To transfer the format into the uniform type, we added ρ_a in the denominator. By adopting Equation (20), the developed heat and mass transfer model for dehumidification/regeneration could predict the air outlet temperature, humidity and solution outlet temperature accurately with absolute discrepancies less than 5%.

(2) Qi correlation [71]

Qi [71] proposed an empirical correlation for an internal heating regenerator by adopting a LiCl solution based on experimental findings. In their test bench, the falling film of liquid desiccant flowed downward and both hot water and air flowed upward. The correlation is shown by Equation (21) as follows:

$$h_m \frac{d_a}{D_a \rho_a} = 3.2\times10^{-4} Sc_a^{0.33} \mathrm{Re}_a^{0.37}\ Sc_s^{0.33} \mathrm{Re}_s^{0.47} \tag{21}$$

The deviations between the experimental results and calculated ones were approximately $\pm 30\%$.

(3) Liu et al. correlation [72]

Liu et al. [72] analysed the heat and mass transfer performance in an internal cooling/heating dehumidifier/regenerator made of thermally conductive plastics for the purpose of corrosion

resistance. A LiBr solution was adopted as the liquid desiccant and cross-flow between the air and the solution was arranged. Based on the experimental results, correlations for volumetric mass transfer coefficient were proposed and are presented in Equation (22).

$$\begin{aligned} h_{m,v} &= 241.3 T_w^{-1.336} m_a^{-0.035} m_s^{0.30} m_w^{0.038} \qquad \textit{Dehumidification} \\ h_{m,v} &= 1766.4 T_w^{-1.142} m_a^{0.529} m_s^{0.471} m_w^{0.071} \qquad \textit{Regeneration} \end{aligned} \tag{22}$$

It is worth noting that Equation (22) is the volumetric mass transfer coefficient with the definition shown in Equation (23). The absolute discrepancies between the predicted and measured mass transfer coefficients were mostly less than 20%.

$$h_{m,v} = \frac{m_a (w_{a,i} - w_{a,o})}{V \Delta w} \tag{23}$$

(4) Lee et al. correlation [73]

Lee et al. [73] proposed a *Sh* number correlation to predict the dehumidification performance in a plate-type dehumidifier using a LiCl solution. The flow pattern between the processed air and the solution was cross-flow. For cold water and the solution, the flow pattern was counter-flow. The proposed correlations are shown in Equation (24).

$$\begin{aligned} \frac{h_{m,a} d_{e,a}}{D_a} &= 0.92 \,\mathrm{Re}_a^{0.381} \,\mathrm{Re}_s^{0.269} \, Sc_a^{0.601} (X_s / X_s^*)^{0.143} (w_a / w_e)^{0.69} \qquad \textit{air side} \\ \frac{h_{m,s} d_{e,s}}{D_s} &= 0.06 \,\mathrm{Re}_s^{0.156} \,\mathrm{Re}_a^{0.313} \, Sc_s^{0.099} (X_s / X_s^*)^{1.133} (w_a / w_e)^{4.462} \qquad \textit{solution side} \end{aligned} \tag{24}$$

In Equation (24), the definitions for the mass transfer coefficients in air and in the solution side are different and expressed by Equation (25). The correlation gave a rational prediction of the air-side Sherwood number within discrepancies of less than $\pm 30\%$.

$$\begin{aligned} h_{m,a} &= \frac{m_a (w_{a,i} - w_{a,o})}{\rho_a A (w_{a,i} - w_e)} \\ h_{m,s} &= \frac{m_a (w_{a,i} - w_{a,o})}{\rho_s A \Delta X_s} \end{aligned} \tag{25}$$

(5) Dong et al. correlation [74]

Dong et al. [74] compared the dehumidification performance of internal cooling dehumidifiers with and without a superhydrophilic coating. Counter-flow between the processed air and a LiCl solution was arranged in their experiments. Correlations for the mass transfer coefficients are shown in Equation (26).

$$h_m = 7.98\times10^4 m_a^{0.686} m_s^{0.250} T_a^{-1.78} T_w^{-0.527} w_a^{0.996} \quad \textit{normal dehumidifier}$$
$$h_m = 3.15\times10^4 m_a^{0.972} m_s^{0.229} T_a^{-0.379} T_w^{-0.375} w_a^{0.012} \quad \textit{coated dehumidifier} \tag{26}$$

Most of the calculated mass transfer coefficients fell within ±25% of the experimental data and the average relative deviations were −0.9% and −1.09% for normal and coated dehumidifiers, respectively.

(6) Wen et al. correlation [13, 75]

Wen et al. [13, 75] experimentally investigated the dehumidification and regeneration performance of an internal heating falling-film regenerator by the liquid desiccant of LiCl solution. The flow pattern between the solution and the regenerated air was counter-flow. Based on the experimental data, they proposed correlations to predict the mass transfer performance and the correlations are shown as follows by Equation (27):

$$Sh_a = 65.1 * Re_a^{-0.62} * Sc_a^{-23.6} * w_{a,i}^{1.57} w_e^{-0.13} \quad \textit{Dehumidification}$$
$$Sh_a = 0.0139 * Re_a^{0.75} * Sc_a^{4.81} * w_{a,i}^{-0.53} w_e^{-0.68} \quad \textit{Regeneration} \tag{27}$$

The absolute relative deviations between the experimental and calculated values for Sherwood number were less than 8%.

Table 5 lists detailed information for internal cooling/heating dehumidifier/regenerators, which includes flow patterns, liquid desiccants and operating parameters.

It is worth noting that the correlations summarised in Section 3.1 are mostly based on experimental results. In fact, during the investigation of dehumidification/regeneration, some researchers also adopted Reynolds analogy for determination of the mass transfer coefficient [76-78]. Reynolds analogy assumes that the heat and mass transfer in a dehumidifier/regenerator are coupled with each other and follow the relationship given in Equation (28).

$$\frac{Nu}{Sh} = Le^n \tag{28}$$

where Nu is the Nusselt number and Le is the Lewis number. Because the correlation of the Nusselt number can be easily obtained from previous research on heat transfer performance, the mass transfer coefficient, which is related to Sh, can also be acquired subsequently.

Table. 5. Summary of mass transfer coefficient correlations for internal cooling/heating types.

Authors	Mode[a]	Flow pattern[b]	Desiccant	Conditions[c]	Accuracy[d]
Yin et al. [70]	D, R	Pr, Pr	LiCl	V_a:1.5-4; T_a:21-32; w_a:6-14.5	≤ 5%

				m_s :0.1-0.12; T_s :20-78; X_s :32-40	
Qi [71]	R	Co, Co	LiCl	T_a :25-50; w_a :5-15; T_s :30-50; X_s :25-30	±30%
Liu et al. [72]	D, R	Cr, Cr	LiBr	m_a :0.118-0.235; T_a :15.1-36.3; w_a :6.8-24.6 m_s :0.017-0.062; T_s :20.6-31.5; X_s :38.8-42.6 T_w :11.1-41.8	±20%
Lee et al. [73]	D	Cr, Co	LiCl	V_a :0.2-1.2; T_a :35; w_a :21.4-28.9 m_s :0.0007-0.0015; T_s :43; X_s :35-45 m_w :0.0015; T_w :32	±30%
Dong et al. [74]	D	Co, Cr	LiCl	m_a :0.027-0.07; T_a :23.6-38.7; w_a :10.9-26.2 m_s :0.01-0.049; T_s :23.1-30.5 m_w :0.03-0.1; T_w :15.6-24.9	Nearly 1%
Wen et al. [13, 75]	R	Co, Co	LiCl	m_a :0.02-0.07; T_a :28-35; w_a :13-23 m_s :0.08-0.15; T_s :24-55; X_s :31-38 m_w :0.12; T_w :15-58	≤ 8%

a: D: dehumidification; R: regeneration;
b: Pr: parallel flow; Co: counter-flow; Cr: cross-flow;
c: m_a , m_s (kg/s); T_a , T_s , T_w (°C); V_a (m/s); w_a (g/kg); X_s (%)
d: a single percentage, such as 5%, means the average discrepancy. A percentage with top and bottom limitations, such as ±30% , means most of the discrepancies fall within this error band.

Attempts were also made to collect usable experimental data for empirical correlation evaluation for the internal cooling/heating type. However, owing to unclear descriptions of equivalent diameter and relevant experimental conditions, it was quite difficult for us to adopt these data to evaluate the correlations. Consequently, we compared the *Sh* number predicted by these correlations under the operating conditions shown in Table 6, just as we did for the adiabatic type. It is noteworthy that the range of the conditions shown in Table 6 was determined according to the literature. The internal cooling dehumidifier was assumed to be a cube with a length of 0.5 m and an equivalent diameter of 0.02 m. The detailed comparison results are presented in Fig. 7.

Table. 6. Operating conditions of different parameters.

Parameter	Ta (°C)	m_a (kg/s)	d_a (g/kg)	T_s (°C)	m_s (kg/s)	X_s (%)	T_w (°C)	m_w (kg/s)
Value	25-39	0.2-1.6	15-24	15-36	0.5-4.0	0.3-0.54	15	1.5

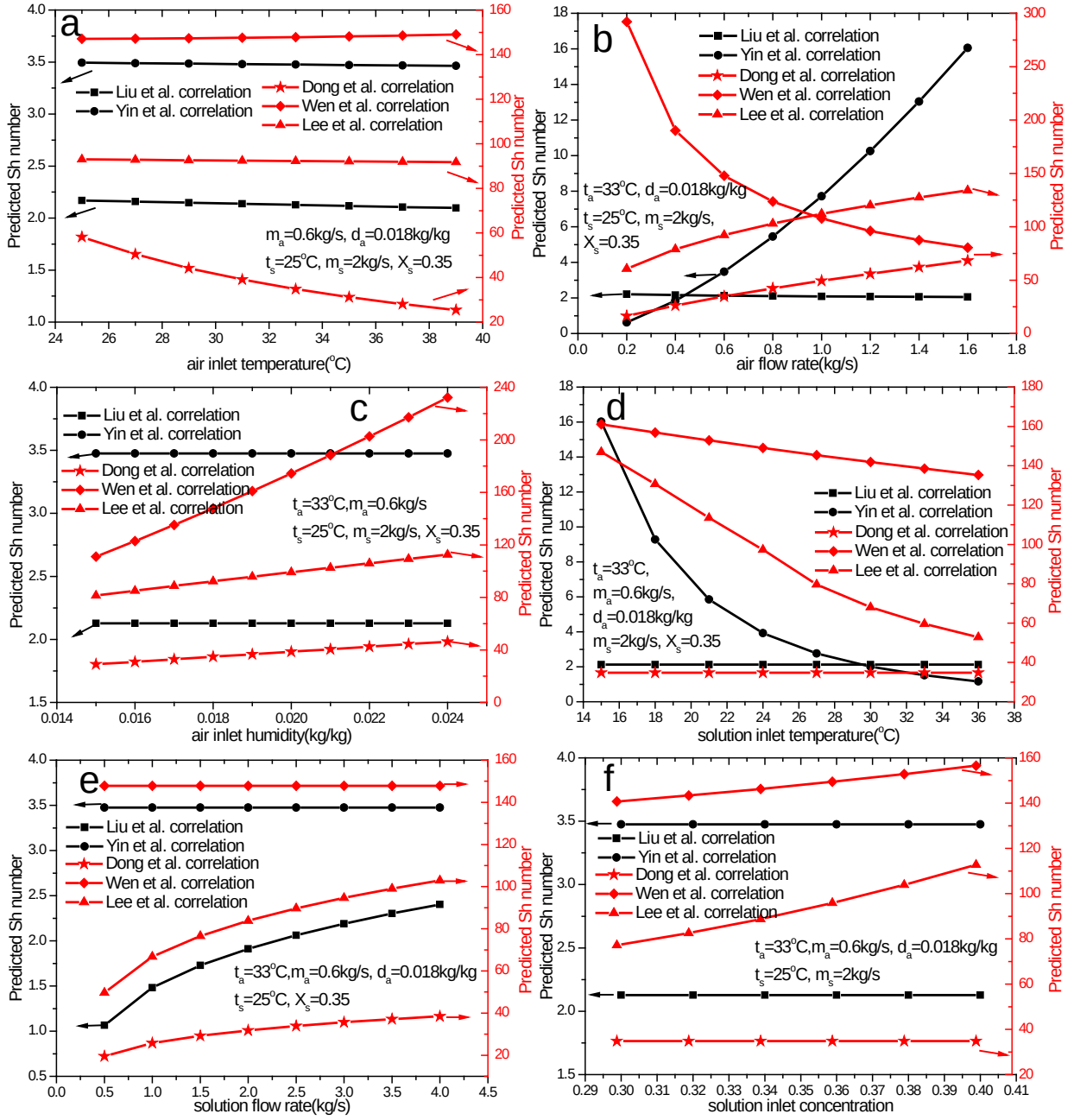

Fig. 7. Comparison of *Sh* number between different correlations for internal cooled dehumidifiers.

It is obvious that the magnitude of the *Sh* number calculated by different correlations varies across a wide range. Moreover, the trends of the curves are different from each other, even under the same operating conditions, which means that the influences of different factors on mass transfer performance are different. For example, in Fig. 7d, the *Sh* number remains almost constant under various solution temperatures for the Liu et al. [72] and Dong et al. [74] correlations. However, ascending trends are observed for the other three correlations. Therefore, in a future study, it will be necessary to investigate the influences of different factors on mass transfer performance in

detail. Moreover, it is also helpful and necessary to indicate the structural parameters of the component in the related material or papers.

3.2 Moisture effectiveness

(1) Chung correlation [79]

Chung [79] developed a correlation of moisture effectiveness for various random packings and liquid desiccants.

$$\eta_m = \frac{1-\left\{\dfrac{0.205(G_a/G_s)^{0.174}\exp[0.985(T_{a,i}/T_{s,i})]}{(aZ)^{0.184}(1-P_s/P_w)^{1.68}}\right\}}{1-\left\{\dfrac{0.152\exp[-0.686(T_{a,i}/T_{s,i})]}{(1-P_s/P_w)^{3.388}}\right\}} \tag{29}$$

The correlation was validated for polypropylene pall rings, ceramic, Berl saddles, glass Raschig rings and polypropylene Flexi rings with the adoption of both LiCl and TEG solutions. The average of the errors between the experimental findings and predicted ones was nearly 7%.

(2) Martin and Goswami [80]

Based on the experimental data for random packed dehumidifiers/regenerators with LiCl or TEG solutions [56, 57, 81-83], Martin and Goswami [80] proposed a dimensionless correlation to calculate the moisture effectiveness, as shown in Equation (30):

$$\eta_m = 1-48.3\left(\frac{G_s}{G_a}\right)^{0.396\frac{\sigma_s}{\sigma_c}-1.57}\left(\frac{h_{a,i}}{h_{s,i}}\right)^{-0.751}(a_tZ)^{0.0331\frac{\sigma_s}{\sigma_c}-0.906} \tag{30}$$

(3) Abdul-Wahab et al. correlation [84]

Abdul-Wahab et al. [84] experimentally identified the moisture removal performance of a TEG solution in structured dehumidifiers with packing densities ranging from 77 to 200 m^2/m^3. According to the statistical analysis of the experimental results, they developed a correlation to calculate the moisture effectiveness, as shown in Equation (31):

$$\eta_m = 0.601+0.257G_s-0.00072a-0.0107T_{a,i} \tag{31}$$

The correlation was applicable for the random packing materials of ceramic Intalox saddles, polypropylene Flexi rings and polypropylene Rauschert Hiflow rings under a wide variety of operating conditions. It predicted the experimental values within $\pm 10\%$ error.

(4) Liu et al. correlation [85, 86]

Liu et al. [85] gave empirical correlations for the prediction of moisture and enthalpy effectiveness based on experimental analysis. Their correlations were suitable for a cross-flow–packed dehumidifier with Celdek structured packing and a LiBr solution.

$$\eta_m = c_1 m_a^{-0.2804} m_s^{0.3657} \tag{32}$$

$$\eta_h = c_0 (h_{a,i} - h_{e,i})^{0.5641} (w_{a,i} - w_{e,i})^{-0.6487} m_a^{-0.4435} m_s^{0.6201} \tag{33}$$

The average absolute differences between the experimental data and predicted ones were 6.0% and 6.3% for moisture effectiveness and enthalpy effectiveness, respectively, with discrepancies mainly within $\pm 20\%$. They also validated the correlations by experimental data from other studies [45, 55, 62] and good agreements were found. In fact, they proposed another dimensionless correlation for the same structure-packed dehumidifier, as shown in Equation (34).

$$\eta_m = \frac{1 - \left\{ \dfrac{0.642 (G_a / G_s)^{0.1} \exp[-0.2 (T_{a,i} / T_{s,i})]}{X_s^{0.537}} \right\}}{1 - \left\{ \dfrac{0.496 \exp[-0.945 (T_{a,i} / T_{s,i})]}{X_s^{1.558}} \right\}} \tag{34}$$

The comparison between the experimental data and predicted ones revealed that 99.4% of the data had discrepancies within $\pm 20\%$ and 83.2% within $\pm 10\%$.

(5) Moon et al. correlation [87]

Moon et al. [87] conducted experiments to investigate the dehumidification performance of a structure-packed tower with the adoption of a $CaCl_2$ solution. The packing material was made of cross-corrugated cellulose paper sheets. The correlation was given as follows:

$$\eta_m = \frac{1 - \left\{ \dfrac{0.363 (m_a / m_s)^{-0.038} \exp[1.012 (T_{a,i} / T_{s,i})]}{(1 - P_s / P_w)^{0.342}} \right\}}{1 - \left\{ \dfrac{0.267 \exp[1.401 (T_{a,i} / T_{s,i})]}{(1 - P_s / P_w)^{0.363}} \right\}} \tag{35}$$

The correlation fit the experimental data well under a wide range of operating conditions with discrepancies within $\pm 10\%$.

(6) Gao et al. correlation [88]

Gao et al. [88] established a cross-flow packed-bed dehumidifier with Celdek structured packing and investigated its dehumidification performance with a LiCl solution. Empirical

correlations for moisture and enthalpy effectiveness were advanced via regression analysis, as shown in Equations (36) and (37).

$$\eta_m = 0.67 m_a^{-0.352} m_s^{0.403} \tag{36}$$

$$\eta_h = 0.015(h_{a,i} - h_{e,i})^{0.831}(w_{a,i} - w_{e,i})^{-0.537} m_a^{-0.483} m_s^{0.712} \tag{37}$$

Equations (36) and (37) are very similar to Equations (32) and (33) proposed by Liu et al. [85] except for the differences in the constants for different parameters. 91.2% of the experimental data were within $\pm 10\%$, with an average discrepancy of 4.5%.

(7) Wang et al. correlation [89]

Wang et al. [89] experimentally identified the dehumidification performance of a structured packed dehumidifier using a LiCl solution. Empirical correlations for moisture and enthalpy effectiveness were proposed and validated by their own experimental data and the results from Fumo and Goswami [55]. The absolute average discrepancy between the measured and predicted values were 5.16% and 5.00% for moisture and enthalpy effectiveness, respectively. The correlations are given as follows:

$$\eta_m = 3.5823 m_s^{0.256} T_{s,i}^{-0.634} w_{a,i}^{0.350} m_a^{-0.322} T_{a,i}^{-0.327} \tag{38}$$

$$\eta_h = 0.5644 m_s^{0.324} T_{s,i}^{-0.540} X_s^{-0.504} m_a^{-0.375} T_{a,i}^{0.274} \tag{39}$$

Table 7 summarises the specifications for these correlations in terms of flow pattern, type of liquid desiccant, operating conditions and prediction accuracies.

Table. 7. Summary of moisture effectiveness correlation.

Authors	Mode[a]	Flow pattern[b]	Desicc-ant	Conditions[c]	Accuracy[d]
Chung [79]	D	Co, R	LiCl TEG		7%
Martin and Goswami [80]	D, R	R	LiCl TEG	G_s / G_a :3.5-15.4; $a_t Z$:84-262; $h_{a,i} / h_{s,i}$:0.4-1.9; γ_s / γ_c :0.8-3.2	±15%
Abdul-Wahab et al. [84]	D	Co, S	TEG	G_a :1.5-2.613; T_a :25-45 m_s :0.13-1; T_s :28-45; X_s :93-98	±10%
Liu et al. [85, 86]	D	Cr, S	LiBr	m_a :0.31-0.47; T_a :24.7-33.9; w_a :10-21 m_s :0.3-0.64; T_s :20.1-29.5; X_s :42.6-54.8	6.0%
Moon et al. [87]	D	Cr, S	$CaCl_2$	G_a :0.8-2.1; T_a :26-40; w_a :16-25 m_s :0.008-0.055; T_s :25-38; X_s :33-43	±10%
Gao et al.	D	Cr, S	LiCl	m_a :0.08-0.14; T_a :27-38; w_a :9.3-21.3	4.5%

[88]				m_s :0.1-0.26; T_s :22-50; X_s :32-40	
Wang et al. [89]	D	Co, S	LiCl	m_a :0.034-0.082; T_a :25-40.5; w_a :10.6-25.1 m_s :0.023-0.12 T_s :16.4-35.3; X_s :31.7-40.1	5.16%

a: D: dehumidification; R: regeneration;

b: Co: counter-flow; Cr: cross-flow; S: structured packing; R: random packing;

c: m_a , m_s (kg/s); T_a , T_s , T_w (°C); w_a (g/kg); X_s (%)

d: a single percentage, such as 5%, means the average discrepancy. A percentage with top and bottom limitation, such as ±30% means most of the discrepancies fall within this error band.

For the dehumidification effectiveness, 148 data points from six different sources were collected and used to evaluate the correlations. The detailed information of data sources and the evaluation results are specified in Table 8. According to Table 8, it is obvious that most of the correlations can only predict the effectiveness accurately based only on their experimental data. However, the correlations developed by Gao et al. [88] and Wang et al. [89] show desirable accuracy for all data points, especially for that developed by Wang et al. [89]. The detailed comparisons between the experimental and calculated effectiveness for the best two correlations of Gao et al. [88] and Wang et al. [89] are displayed in Fig. 8. The MARD, which is defined by Equation (40), is only 15.2% for all data, regardless of the type of solution and flow pattern.

$$MARD = \frac{1}{N}\sum_{i=1}^{N}\left|\frac{\eta_{m,cal} - \eta_{m,\exp}}{\eta_{m,\exp}}\right| \tag{40}$$

Table. 8. Evaluation of correlations by different data sources.

Data source	Number of data points	Solution	Flow pattern	MARD of different correlations (%)					
				Chung	Abdul-Wahab	Liu	Moon	Gao	Wang
Wang et al. [89]	39	LiCl	counter	28.5%	96.2%	41.6%	12.8%	22.2%	9%
Liu et al. [85]	24	LiBr	cross	22.1%	39.3%	7.3%	16%	22.9%	17.8%
Fumo et al. [55]	14	LiCl	counter	29.6%	142.3%	235.2%	14.5%	59%	6.2%
Chen et al. [90]	9	LiCl	cross	25.8%	77.3%	79.1%	34.5%	25.7%	39.1%
Zhang et al. [63]	25	LiCl	cross	165%	87.8%	73%	146%	16.6%	25.1%
Gao et al. [88]	37	LiCl	cross	26.2%	49.6%	53.6%	12.4%	30.5%	10.8%
Final	148			48.9%	77.1%	64.9%	37.2%	27.1%	15.2%

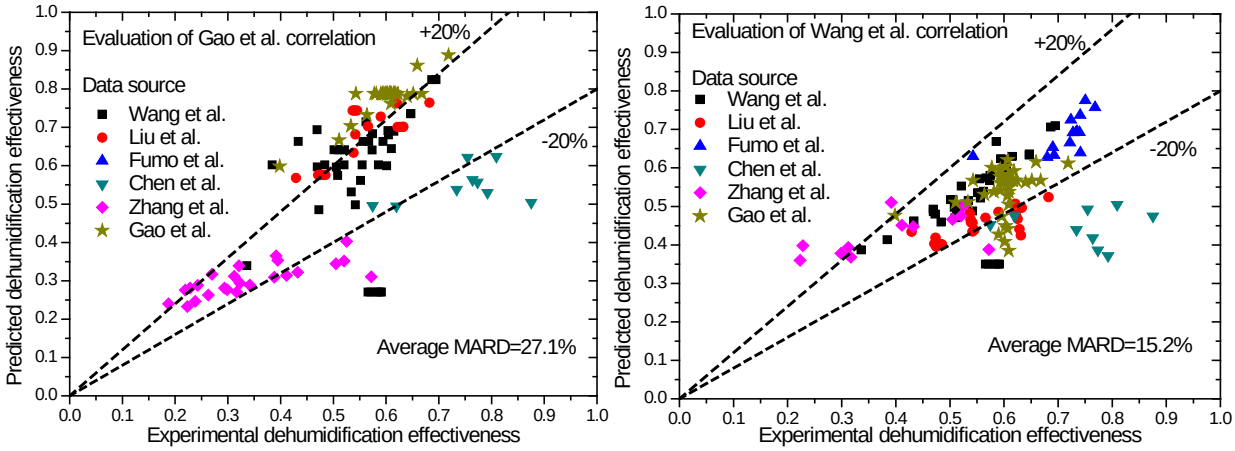

Fig. 8. Comparison between the experimental and predicted effectiveness of Gao et al. [88] and Wang et al. [89] correlations.

4 Enhancement approaches by structural improvement

4.1 Enhanced structures

The random-packed bed was first used as a dehumidifier/regenerator in LDCS. Packing materials without regular geometric configurations such as pall rings and ladder rings are placed randomly in the packing column. The random placement of packing materials could result in undesirable and uncontrollable distribution of liquid desiccant on the surface. Moreover, problems such as wall flow and channel flow may occur under low solution flow rates [34]. The flow resistance of air in the column is usually high, which corresponds to the high power consumption of air fans. To overcome such drawbacks, structure-packed beds with higher efficiency and smaller flow resistance of air were developed [34]. Factors such as volumetric area, void volume and space interval play important roles in the determination of heat and mass transfer performance [40]. The main method to enhance the heat and mass transfer performance in a structure-packed bed is structural optimisation. Some new kinds of structured packing materials with high specific surface areas and special configurations such as corrugated cellulose type [85-87], plant fibre type and Z-type [68] have been used to get desirable dehumidification/regeneration performance, as shown in Fig. 9.

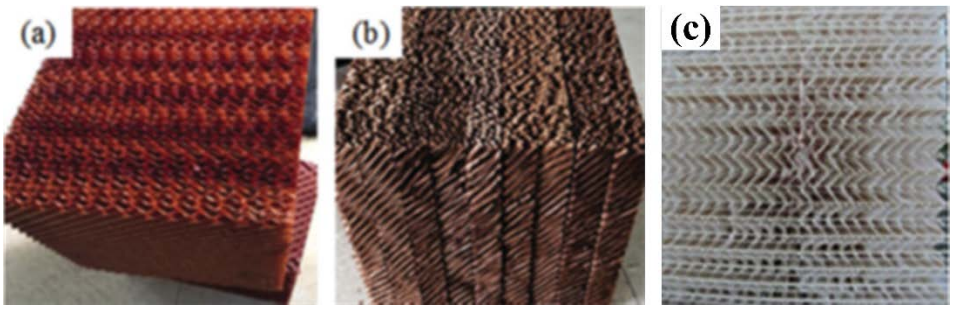

Fig. 9. Structured packing materials: (a) Corrugated cellulose type, (b) plant fibre type and (c) Z-type.

Because of the latent heat release/absorption during dehumidification/regeneration, the solution temperature increased/decreased gradually, which greatly deteriorated the mass transfer performance. Therefore, researchers developed the internal cooling/heating type to overcome the temperature variation by introducing an extra cold/heat source. The dehumidifier/regenerator with internal cooling/heating is usually built up in the form of a falling film, as shown in Fig. 10. Compared with the packed-bed type, the falling-film dehumidifier/regenerator can be easily integrated with internal cooling/heating for high efficiency. Moreover, as the liquid desiccant flows in the form of a falling film, the possibility of liquid carryover decreases. At the same time, the pressure drop at the air side will also decrease if falling type is adopted. Owing to its promising application prospects, emphasis is put on this type of dehumidifier/regenerator in this paper.

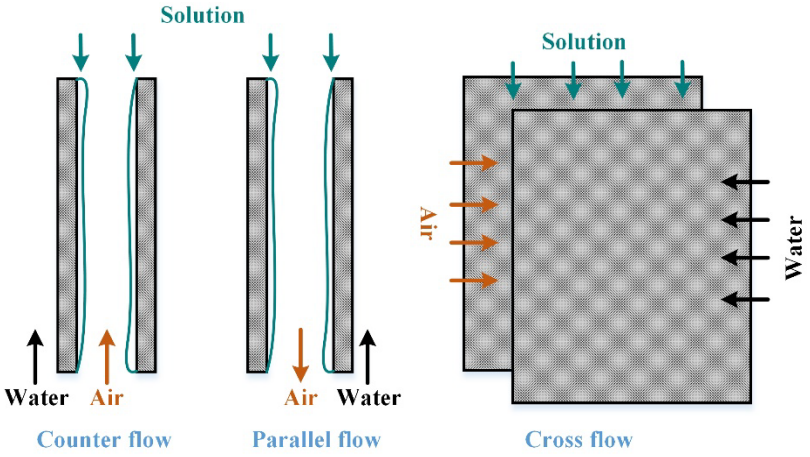

Fig. 10. Schematic diagram of falling film type.

Yin et al. [91] designed a new kind of internal cooling/heating dehumidifier/regenerator based on the plate-fin heat exchanger (PFHE), which is shown in Fig. 11. The assembled unit contained six PFHEs stacked along the vertical direction. Experimental results revealed that the internal heating regenerator showed better performance in terms of regeneration efficiency and thermal performance than an adiabatic one. Khan [92] numerically investigated the absorption

performance of a finned-tube dehumidifier with internal cooling, as shown in Fig. 12. The influencing factors on absorption performance were quantitatively analysed. However, no further experimental work was conducted to validate their findings. Zhang et al. [93] experimentally examined the dehumidification performance of an internal cooling tube-fin dehumidifier made of stainless steel, as shown in Fig. 13. They systematically identified the influences of various inlet parameters on the dehumidification performance by adopting a LiBr solution. Luo et al. [25] also experimentally and theoretically identified the dehumidification performance of a fin tube-type dehumidifier with internal cooling. In this case, the dehumidifier was electroplated to cover some antiseptic materials on its surface for the purpose of corrosion resistance. The flow pattern between the solution and the processed air was arranged to be cross-flow. A photograph of the dehumidifier is shown in Fig. 14. Compared with other dehumidifiers in previous studies, they found that the adopted one performed well in terms of moisture effectiveness. Moreover, their immersion corrosion tests indicated that both the stainless steel 304 and copper could not resist corrosion by the liquid desiccant, as shown in Fig. 15a. The test results from Wen et al. also indicated the causticity of the LiCl solution on aluminium, as shown in Fig. 15b. Even though the metal-based dehumidifier/regenerator has good wettability and structural strength, the metal corrosion would greatly reduce the system reliability and affect the heat and mass transfer performance. Consequently, previous investigators put forward some methods to reduce the corrosion rate in terms of surface treatment [25, 27] and new material development [94, 95]. Liu et al. [72] fabricated a fin-tube dehumidifier with internal cooling by using a thermally conductive plastic for the purpose of corrosion resistance, as shown in Fig. 16. The thermal conductivity of the plastic was as high as 16.5 W/(m·K) and the specific surface area of the dehumidifier reached 342 m^2/m^3. Compared with the internal cooling dehumidifier made of metals, the plastic one showed comparable heat and mass transfer performance during dehumidification, which is a promising alternative for the metal-based dehumidifier/regenerator. Lee et al. [73] designed a plate-type internal cooling dehumidifier by heat-resistant ABS (XR-474). To improve its wettability, a hydrophilic coating was applied and some grooves were carved on its surface, as shown in Fig. 17. The influences of different parameters on dehumidification performance were experimentally identified, and a new *Sh* number correlation was proposed.

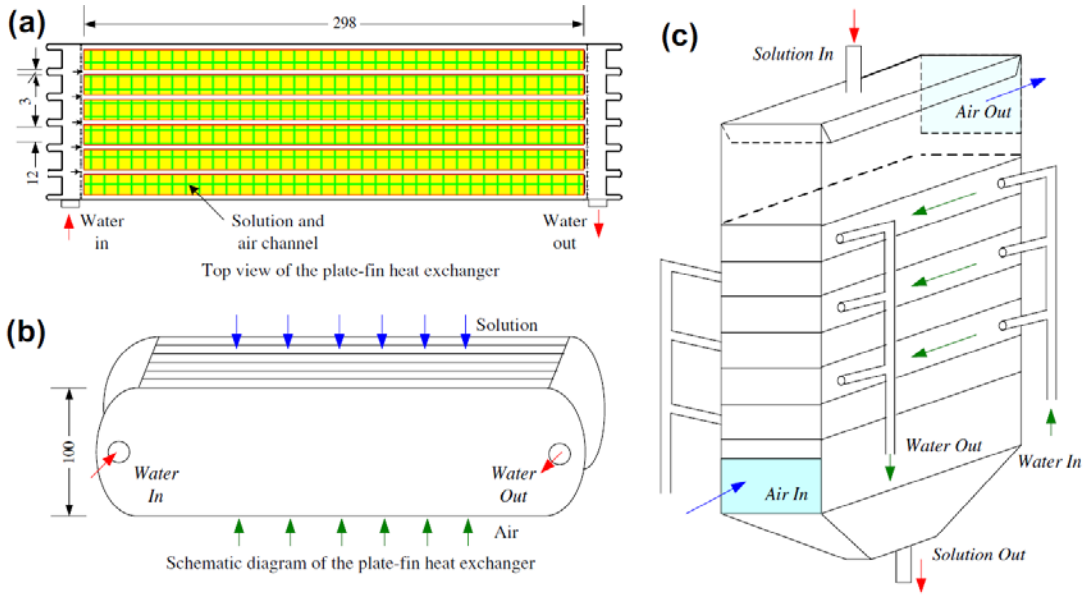

Fig. 11. Schematic diagram of the internal cooling/heating dehumidifier/regenerator [91].

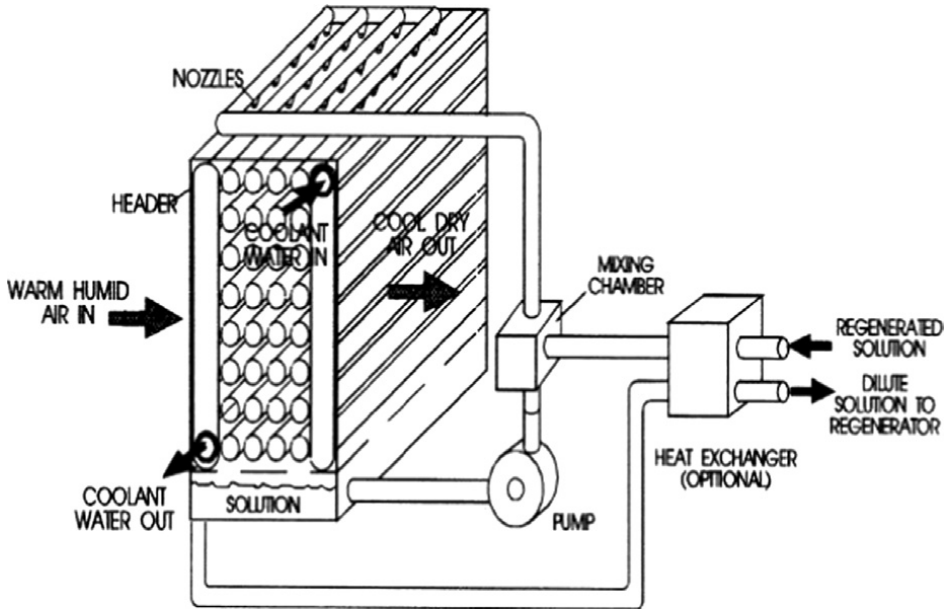

Fig. 12. Schematic diagram of internal cooling fin-tube dehumidifier [92].

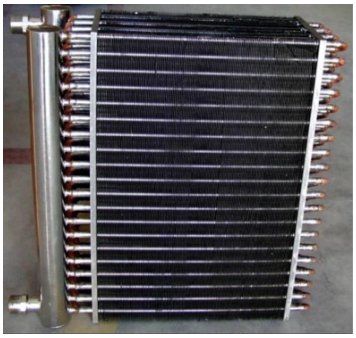

Fig. 13. Photograph of the fin-tube internal cooling dehumidifier made of stainless steel [93].

Fig. 14. Photograph of the fin-tube internal cooling dehumidifier [25].

Fig. 15. Corrosion phenomenon of liquid desiccant on metals [26].

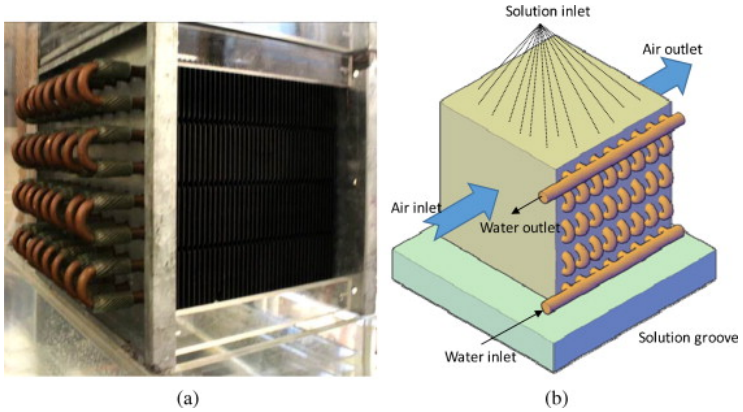

Fig. 16. Photograph and schematic diagram of the dehumidifier made of plastic [72].

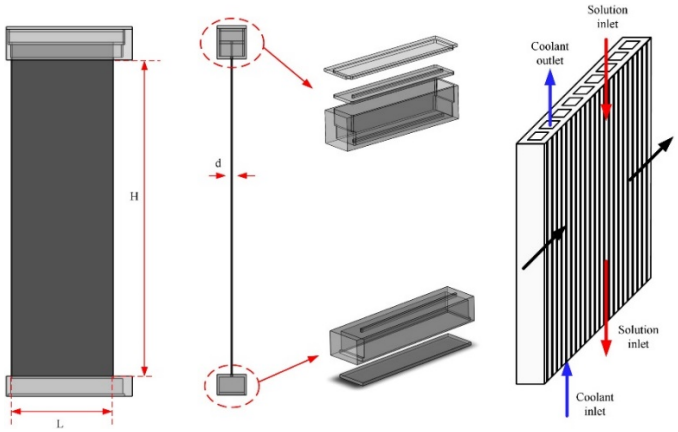

Fig. 17. Schematic diagram of the heat-resistant ABS based dehumidifier [73].

Because the absorption refrigeration operates in a manner similar to liquid desiccant dehumidification, some mass transfer enhancement methods for the absorption refrigerant are also reviewed. Isshiki and Ogawa [96] investigated the heat and mass transfer performance in tube absorbers with the adoption of so-called constant curvature surface (CCS) tubes, as shown in Fig. 18. By adopting the CCS tubes, the falling-film thickness could be maintained at a relatively constant value, and the wetting characteristics performed well in both vertical and horizontal tube absorbers. The authors indicated that the improvement in heat transfer coefficient and mass transfer coefficient were in the range of 0%–40% and 0%–70%, respectively, for several CCS tubes. Similarly, Yoon et al. [97] and Park et al. [98] proposed some tube-based absorbers with special structures, such as bumping tubes, floral tubes, twisted floral tubes [97] and micro-scale hatched tubes [98], to enhance the absorption performance. Their results showed that the floral tube and twisted floral tube increased the heat and mass transfer performance up to 40% compared with a bare tube. The absorption performance of micro-scale hatched tubes was up to two times higher than that of the bare tube.

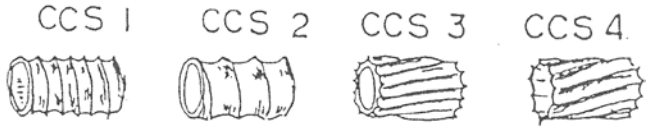

Fig. 18. Examples of CCS tubes [99].

Islam et al. [100] introduced a novel absorber design concept called the film-inverting absorber. Conventional horizontal tubes or plate absorbers were modified to change the continuous film into a repeatedly inverting film, as shown in Fig. 19. The two proposed absorbers were tested experimentally under various conditions. The maximum increase of absorption rate for the film-inverting absorber was about 100% compared with that of the tubular absorber. Similar to Islam's work [100], Cui et al. [101] applied the film invertor idea to a plate absorber with the same consideration of Islam [100], as shown in Fig. 20. Mortazavi et al. [102] designed and fabricated a absorber with a plate-fin structure, as shown in Fig. 21. To achieve better surface wetting, special surface treatments with both physical and chemical methods were introduced. Experimental data with significant high absorption performance were achieved in comparison to the traditional absorption system.

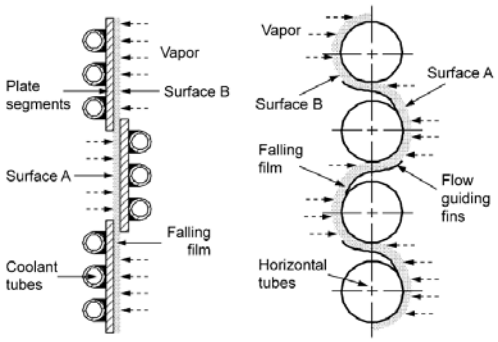

Fig. 19. Film-inverting absorbers [100].

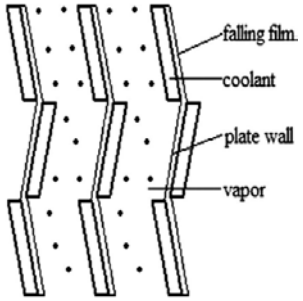

Fig. 20. Film-inverting plate absorber [101].

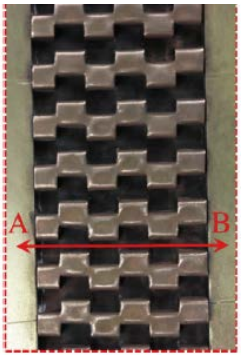

Fig. 21. Absorber made of plate with offset fins [102].

4.2 Surface modification

The non-wettability of a falling film on the surface of a dehumidifier/regenerator has been mentioned by previous studies [76, 103, 104]. Fig. 22 shows an infrared picture of a falling film on a plate-type dehumidifier. As one can see, the falling film shrinks gradually along the flow direction, which results in a decrease of the wetting area and thus a reduction of heat and mass transfer performance during dehumidification/regeneration. To overcome or alleviate the film

contraction, researchers have tried to modify the surfaces of the packing materials or plates both physically and chemically.

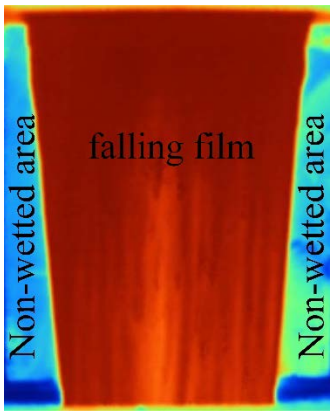

Fig. 22. Shrinkage of falling film on plate.

As mentioned above, Mortazavi et al. [102] modified the surface of the plate absorber with offset fins by physical and chemical methods. Physically, the fins were first sandblasted with fine aluminium oxide particles to form microscale surface roughness. Chemically, the fins were oxidised in boiling water for 5 h; thus, the contact angle of the LiBr solution on the fin decreased from 90° to 30° (shown in Fig. 23), which corresponded to the improvement of wettability of the falling film on the absorber. Wang et al. [105] discontinuously coated the tube absorber by fluorocarbon layers of polyperfluoroalkoxylether (PFA) and polytetrafluoroethylene (PTFE), as shown in Fig. 24. Their motivation was that such arrangements could enhance the mixing of the solution and thus the heat and mass transfer process during absorption. Their experimental results verified that the divided coated tubes significantly enhanced the heat and mass transfer performance. Qi et al. [106] developed a new approach to enhance the heat and mass transfer performance by coating a titanium dioxide superhydrophilic self-cleaning dispersed paste onto the dehumidifier surfaces. The contact angles of the LiBr solution on the coated surfaces significantly decreased to only one sixth compared to the uncoated samples, as shown in Fig. 25. Numerical simulation indicated that the moisture removal rate and heat exchange rate between the LiBr solution and the processed air increased by 1.2 and 2 times, respectively. Dong et al. [74, 107] experimentally investigated the dehumidification performance of an internal cooling dehumidifier coated with a TiO_2 superhydrophilic coating. The contact angle of the LiCl solution on the dehumidifier decreased dramatically from 84.6° to 8.8°, as shown in Figs. 26a and 26b. The experimental results showed that the dehumidification performance was significantly enhanced,

with average enhancing ratios of 1.60 for moisture removal rate and 1.63 for dehumidification efficiency.

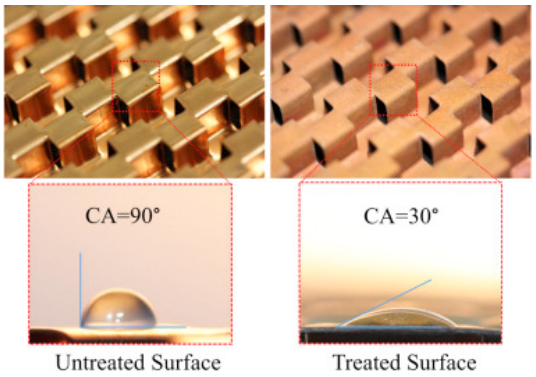

Fig. 23. Contact angle of LiBr solution on different surfaces [102].

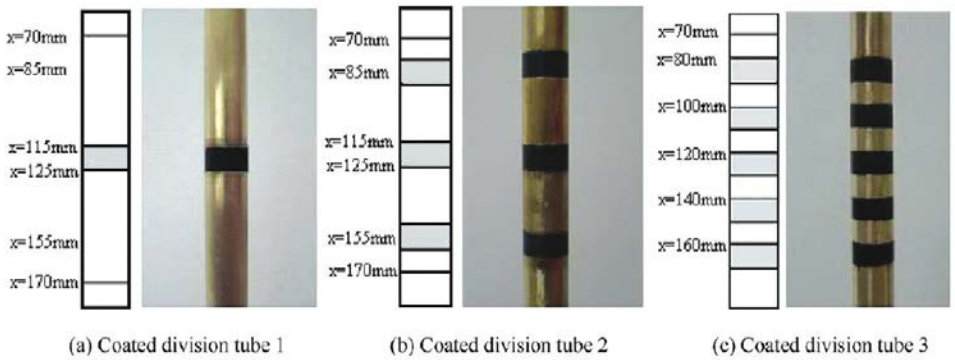

Fig. 24. Surface configurations and dimension for different coated division tubes [105].

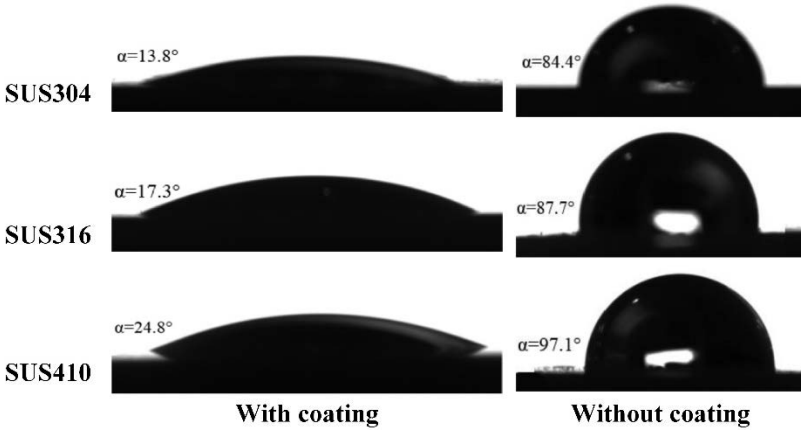

Fig. 25. Contacts of LiBr solution on different surfaces with and without coating [106].

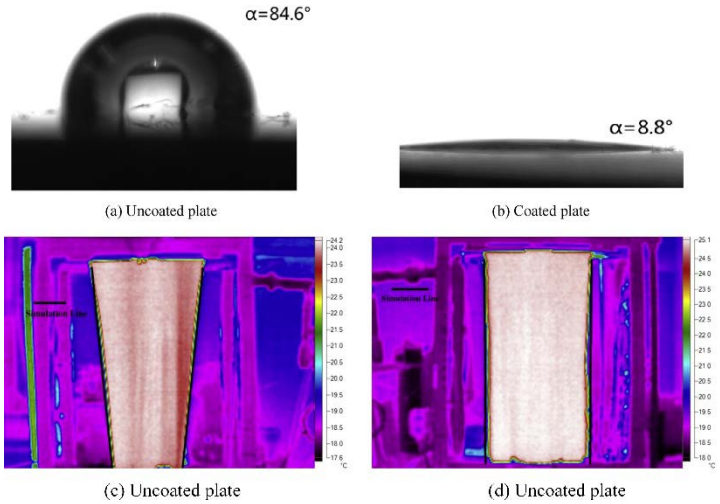

Fig. 26. (a, b) Contact angle [74] and (c, d) wettability of falling film [107] on (a, c) uncoated and (b, d) coated plates.

Some physical methods were also used to improve the wettability of the falling film and heat and mass transfer performance. Hassan et al. [77] proposed a new method to improve the wettability of the surfaces of a cylindrical dehumidifier channel by covering it with fibrous sheets, as shown in Fig. 27. The fibrous sheets helped maintain complete wetting of the heat and mass transfer surfaces through the capillary effect of the fibres. On the one hand, by adopting the fibrous sheets, the surface could be completely wetted. On the other hand, the air pressure drop could also decrease owing to the avoidance of channel blockage by the solution. Lun et al. [108] also covered the surface of a dehumidifier with a hydrophilic fabric (gauze) to achieve high porosity and good surface wettability. However, they added anhydrous ethanol to the LiCl solution for self-cooling. A summary of these enhancement methods by surface modification is specified in Table 9.

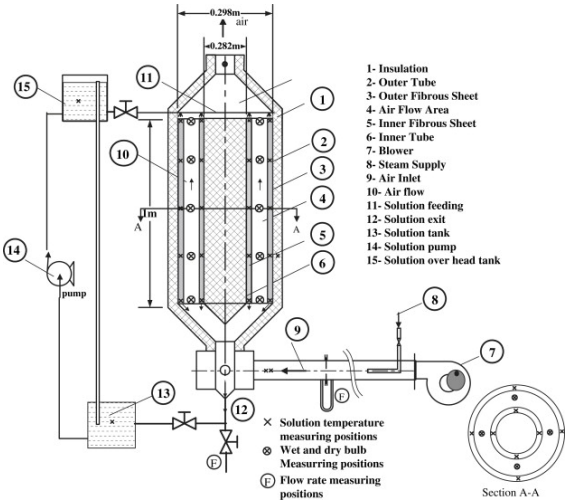

Fig. 27. Experimental setup with fibrous sheets covering the dehumidifier [77].

Table. 9. Summary of mass transfer enhancement by surface modification.

Authors	Mode[a]	Desiccant	Method
Mortazavi et al. [102]	A	LiBr	Surface sandblast, oxidation
Wang et al. [105]	H	Water	Fluorocarbon layer
Qi et al. [106]	D	LiBr	TiO_2 superhydrophilic coating
Dong et al. [74, 107]	D	LiCl	TiO_2 superhydrophilic coating
Hassan et al. [77]	D	$CaCl_2$	Fibrous sheet
Lun et al. [108]	D	LiCl	Hydrophilic fabric

a: A: absorption; H: heat transfer; D: dehumidification

4.3 Ultrasonic atomisation enhancement

When ultrasonic energy with a certain intensity and frequency are imposed on a liquid, cavitation with the violent formation and implosion of a large number of micro-scale vapour bubbles can be induced. Because the implosion of bubbles occurs near or at the surface of the liquid, quite small liquid droplets can be generated and released [109]. The phenomenon is called ultrasonic atomisation. There is a relationship between the ultrasonic frequency, the thermal properties of the liquid and the diameter of the droplets [110].

$$d_m = 2.8\left(\frac{\sigma_s}{\rho_s f^2}\right)^{1/3}\left(\frac{\mu_s}{\mu_w}\right)^{-0.18} \tag{41}$$

where f is the frequency of the ultrasonic energy. It is obvious that the diameter of the droplet decreases with the increasing frequency. Correspondingly, the specific surface area of the liquid desiccant will increase significantly with decreasing droplet diameter. The mass transfer coefficient between the liquid droplets and air can be calculated by Equation (42) when the Reynolds number is less than 400 [111].

$$h_m = \frac{D_a}{d_m}\left[1+\left(Sc_a+\frac{1}{\mathrm{Re}_a}\right)^{1/3}\mathrm{Re}_a^{\,0.41}\right] \tag{42}$$

To clearly illustrate the relationship between droplet diameter and mass transfer coefficient, a figure was plotted by Yao [109] for a LiBr solution according to Equation (42) under various air velocities, as shown in Fig. 28. Based on the above-described theoretical background, an experimental system was built to investigate the liquid desiccant regeneration with ultrasonic atomisation, as shown in Fig. 29 [112]. A hot and weak liquid desiccant was atomised by an ultrasonic atomiser at 30 kHz and sprayed into the atomising chamber. In the chamber, the droplets of liquid desiccant and regeneration air came into contact. After the regeneration process, the weak solution became strong, and most of the liquid droplets fell into the solution tank at the bottom of

the atomising chamber. The rest of the droplets were entrained by the air flow and were intercepted by wire mesh demisters at the outlet of the chamber. Yang et al. [113] both numerically and experimentally studied the regeneration performance of an ultrasonic atomisation liquid desiccant regeneration system. A schematic diagram of the experimental system and the ultrasonic transducer is shown in Fig. 30. The results indicated that the adoption of ultrasonic atomisation could lower the regeneration temperature as much as 4.4 °C. In terms of energy consumption, a considerable energy conservation potential of 23.4% could be achieved with the use of this ultrasonic atomisation liquid desiccant regeneration system. Moreover, the potential could increase up to 60.4% compared with a packed-bed system if an ultrasonic atomisation-assisted dehumidifier was integrated. Yao et al. [114] advanced another kind of ultrasonic atomisation liquid desiccant regenerator, as shown in Fig. 31. Unlike that shown in Figs. 29 and 30, the ultrasonic transducer shown in Fig. 31 was arranged at the bottom of the regeneration chamber, and the liquid droplets were dispersed into the chamber by the intensive vibration and atomisation of an ultrasonic transducer. However, no experimental study was carried out to evaluate the performance.

In addition to investigation of ultrasonic atomisation regenerators, some researchers also studied the performance of ultrasonic atomisation dehumidifiers [115-117]. Wang et al. [115, 116] proposed a new liquid desiccant dehumidification system based on ultrasound atomisation. As the liquid desiccant in the dehumidifier was atomised into fine liquid droplets by the ultrasonic transducer, the heat and mass transfer area between the processed air and the liquid desiccant dramatically increased. The results of a numerical study indicated that the amount of desiccant consumption was reduced remarkably and that the dehumidification performance was good. Yang et al. [117] experimentally investigated the dehumidification performance of an ultrasonic atomisation dehumidification system, as shown in Fig. 32. Similar to the regenerator introduced in Fig. 30, an ultrasonic transducer was used to atomise the liquid desiccant into fine droplets. After optimisation, less liquid desiccant was consumed, with an average reduction of 45.9%. Moreover, the dehumidification performance was significantly improved from 20.8% to 66.5%, and the desiccant concentration could also be reduced if the same dehumidification effectiveness was supposed.

It is obvious that the adoption of ultrasonic atomisation technology in LDCSs can reduce the amount of liquid desiccant consumption and increase the heat and mass transfer performance. However, a considerable and serious problem with the ultrasonic atomisation (i.e., liquid carryover)

must be overcome and avoided before its large-scale application. Because the liquid desiccant is atomised into many fine droplets, it is more likely to be carried into the air-conditioned room by air, which is a great threat to residents' health. Even though the possibility of liquid carryover can be greatly reduced by a mist eliminator, fine droplets are still likely to enter the room. Therefore, rigorous validation for the feasibility of this technology should be carried out before its real application.

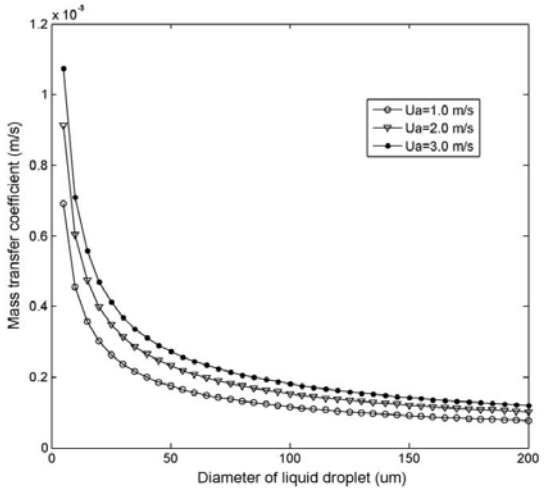

Fig. 28. Mass transfer coefficients between droplet of LiBr solution and air [109].

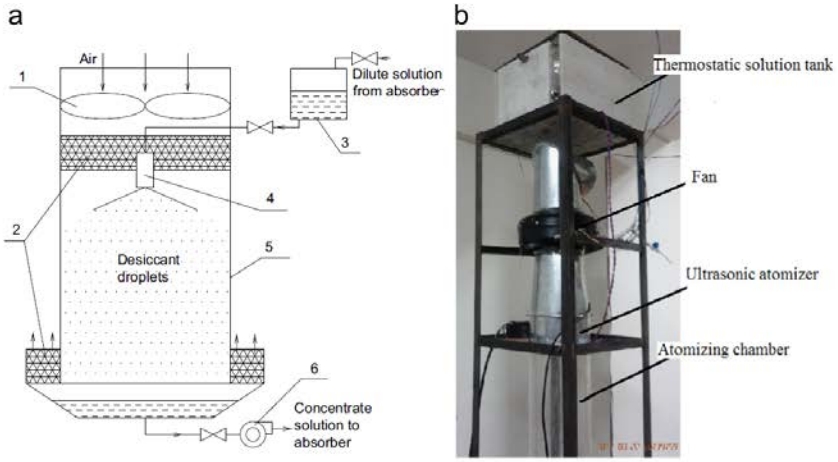

Fig. 29. Schematic and photograph of the liquid desiccant regenerator with ultrasonic atomiser [112].

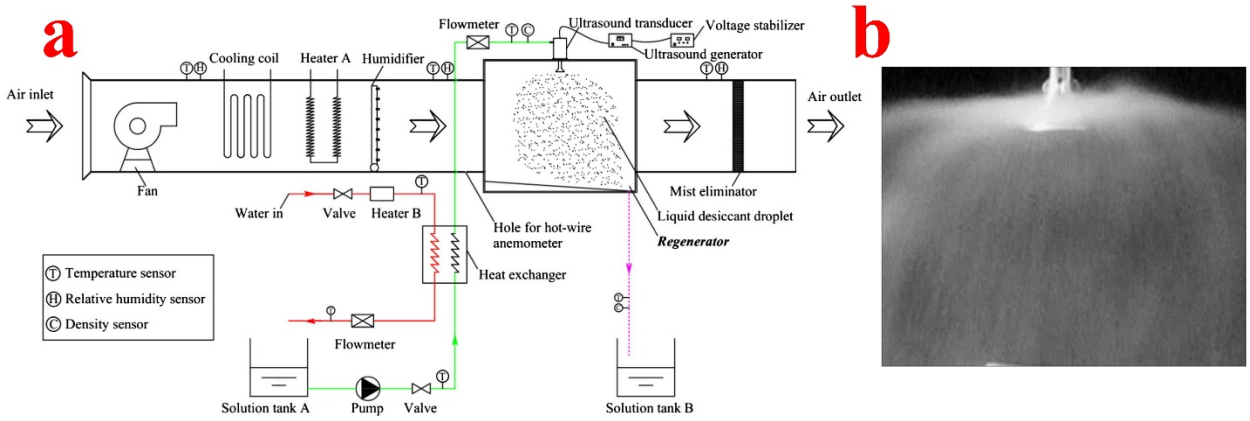

Fig. 30. (a) Schematic diagram of the ultrasonic atomisation LDCS and (b) photograph of liquid droplet generated by ultrasonic transducer [113].

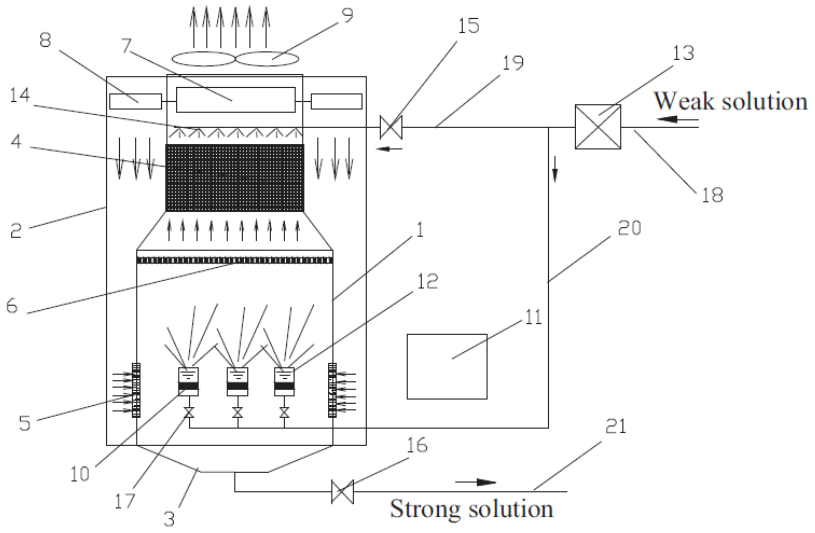

1.Inner wall 2.Outer wall 3.Desiccant solution storage tank 4.Demister 5.Air intake 6.Weir plate 7.Evaporation end of heat pipe 8.Condensation end of heat pipe 9.Exhaust fan 10.Ultrasonic atomizer 11.Ultrasonic generator 12.Atomization tanks 13.Desiccant solution heater 14. Solution sprinkler 15.Solution valve (A) 16. Solution valve (B) 17.Liquid level control valve 18.Inlet liquid pipe 19.Branch liquid pipe (A) 20. Branch liquid pipe (B) 21. Outlet liquid pipe

Fig. 31. Schematic diagram of the liquid desiccant regenerator with ultrasonic atomising [114].

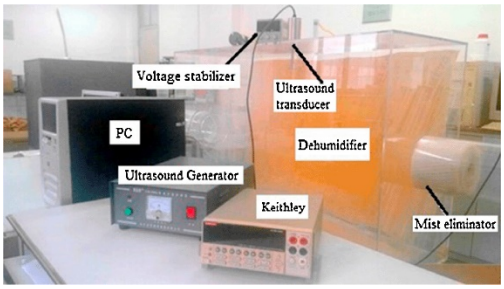

Fig. 32. Photograph of the ultrasonic atomisation dehumidification system [117].

4.4 Membrane-based dehumidifier/regenerator

Even though the plate-type falling-film dehumidifier/regenerator can greatly reduce the possibility of liquid carryover, it is still likely to occur under high air velocity. To thoroughly avoid liquid carryover, researchers developed a membrane-based dehumidifier/regenerator. Other potential benefits, such as a large contact area per unit volume (typically 800 m^2/m^3 for plate type and up to 2000 m^2/m^3 for hollow fibre type), a low pressure drop on the air side and good dehumidification/regeneration efficiency, have also made the membrane-based module draw more and more attention in recent years [118-121].

In a membrane-based LDCS system, special membranes with particular selectivity and permeability are used to separate the humid air and liquid desiccant. The membrane only allows the transformation of water vapour while preventing the solution from crossing over to the air side. Microporous membranes made of polypropylene, polyethylene, polytetrafluoroethylene and polyvinylidene fluoride is often used. However, in practical application, the microporous membrane has the potential risk of pore-wetting by the liquid desiccant [122]. That is to say, the liquid desiccant is likely to penetrate the membrane because the separation between the liquid and the air is not absolute. To reliably avoid such a phenomenon, the microporous membrane is usually coated with other kinds of materials, such as a dense layer of amorphous Teflon, silicone or gel. In fact, the configuration of membrane-based dehumidifier/regenerators is very similar to that of plate-type or shell tube-type heat exchangers in which two fluids flow on two sides of the heat exchanger [123]. Therefore, there are mainly two kinds of membrane modules: plate modules [124, 125] and shell-tube modules [126, 127]. The plate module has a simple structure and is easy to fabricate. However, it has a relatively small packing density. However, the shell-tube module has a greater packing density, which corresponds to better heat and mass transfer performance. Nevertheless, it is difficult to construct because of its complex structure. Moreover, the pressure drop in the module is also higher.

For the plate-type module, theoretically speaking, it has three flow configurations between the solution and the air: parallel flow, counter-flow and cross-flow. However, restricted by the difficulties in construction and sealing, parallel and counter-flow are seldom arranged in the module. A schematic diagram for the cross-flow type module is shown in Fig. 33 [128]. The solution and air flow alternatively in different channels separated by membranes. In fact, because the efficiency of the counterflow module is nearly 10% higher than that of the crossflow type [129],

Vali et al. [130] purposely designed two inlet and outlet headers with cross-flow configurations and combined them with the main module with counter-flow configuration to achieve better performance, as shown in Fig. 34. For the shell-tube module, hollow fibre membranes are used, and in most engineering applications, the solution flows inside the hollow fibre and air flows outside on the shell side, as shown in Fig. 35 [126, 131].

The abovementioned membrane-based modules are all adiabatic, which means that the dehumidification/regeneration performance would deteriorate with the processing of heat and mass transfer owing to solution temperature increase/decrease. To further improve the efficiency, an internal cooling/heating type module was proposed and investigated, as shown in Fig. 36. Huang et al. [132] used an analytical approach to study the dehumidification performance of a plate-type module with internal cooling. They found that the module's dehumidification performance was significantly improved when internal cooling was adopted to keep the solution temperature low. Woods and Kozubal [133] also numerically studied the heat and mass transfer characteristics of a plate-type module with internal cooling. They adopted the Monte-Carlo sensitivity analysis method to identify the influences of various operating parameters.

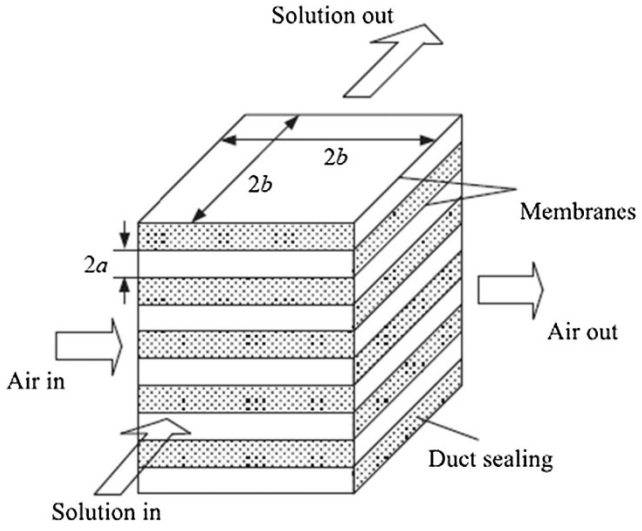

Fig. 33. Schematic diagram of the cross-flow module [128].

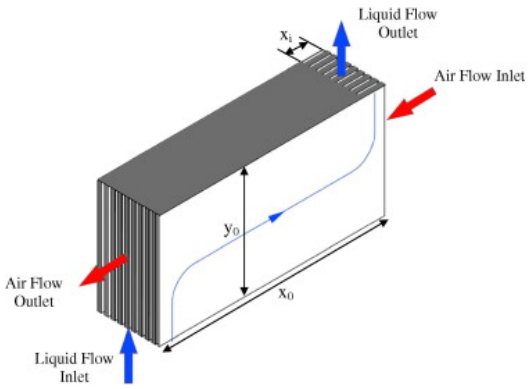

Fig. 34. Schematic diagram of the plate-type counter–cross module [130].

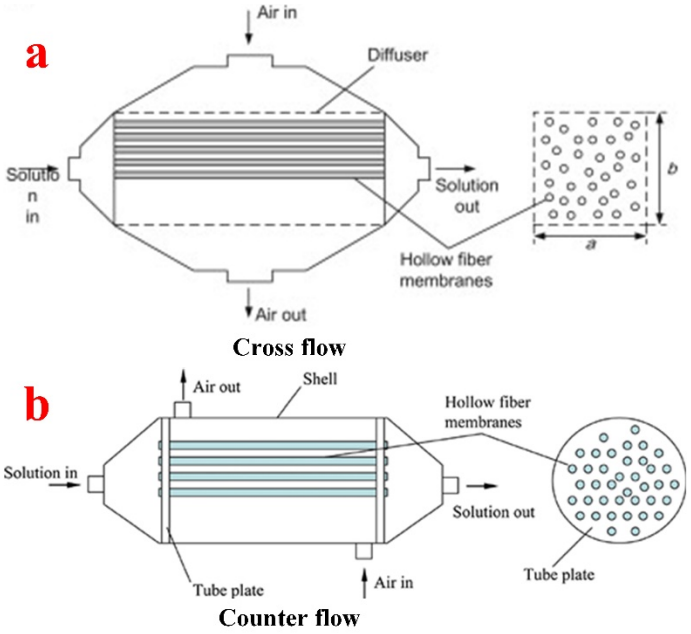

Fig. 35. Schematic diagram of shell-tube module: (a) cross-flow [131] and (b) counter-flow [126].

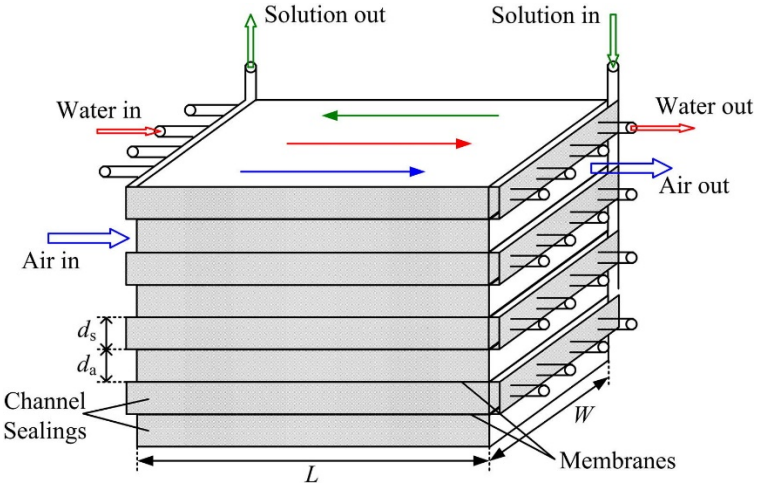

Fig. 36. Structure of an internal cooling plate-type membrane-based dehumidifier [132].

5 Enhancement approaches by solution modification

5.1 Addition of surfactant

Some researchers have attempted to add certain kinds of chemical surfactants into the liquid desiccant to enhance the water vapour absorption efficiency. In the early 1960s, Beutler et al. [134] revealed that the absorption rate of refrigerant vapour could be remarkably enhanced by the addition of certain kinds of alcohols and other hydrocarbon chain compounds with polar groups. In the later 20th century, plenty of research focused on mass transfer enhancement via the addition of surfactants . Cosenza and Vliet [135] investigated the water vapour absorption characteristics by a LiBr solution in a tube falling-film absorber. They found that the absorption rate could be enhanced up to four times by adding the surfactant 2-ethyl-1-hexanol. After that, 2-ethyl-1-hexanol was also used as a surfactant both in plate- and tube-type absorbers [136-139]. Hihara and Saito [136] found a four- to five-fold enhancement in absorption rate in a plate-type LiBr-based absorber. Perez-Blanco and Sheehan [137] revealed that the enhancement ratio was related to the surfactant concentration and that the enhancement could reach up to 35% when adding 1000 ppm 2-ethyl-1-hexanol to a 54.2% LiBr solution. Rivera and Cerezo [138] added both 1-octanol and 2-ethyl-1-hexanol into a 2 kW single-stage heat transformer using a LiBr solution. The results showed that the coefficient of system performance increased up to 40% after adding 2-ethyl-1-hexanol. Sun and Zhang [139] also verified the enhancement of absorption by adding 2-ethyl-1-hexanol. N-octanol and n-decanol were used by Hozawa et al. [140] to study the static absorption performance by a LiBr solution. They found that the initial absorption rate increased up to 2.5 times with the addition of n-octanol. In 1996, Ziegler and Grossman [141] reviewed the progress of heat and mass transfer enhancement by the addition of surfactants. According to the review, the relevant research could be divided into three groups: stagnant pool absorption, vertical and horizontal falling-film absorbers and field tests. The commonly adopted surfactants, such as 2-ethyl-1-hexanol, n-octanol, 6-methyl-2-heptanol and n-heptanol, were introduced, and researchers investigated their influences on heat and mass transfer performance. Kang et al. [142] added Triton X-100 to the water to study the fluid flow and heat transfer performance of falling films on a heated surface. They found that the contact angle of water decreased with the increasing concentration of Triton X-100, which led to an increase in the falling-film wetting area (as shown in Fig. 37) and a decrease in the falling-film thickness. Consequently, the heat transfer rate was significantly increased by adding Triton X-100. Wen et al. [75, 143] added the surfactant PVP to an LiCl solution for the

purpose of mass transfer enhancement in LDCSs. They found that the contact angle of the LiCl solution on a stainless-steel plate initially decreased and then levelled off with the increase of surfactant concentration, as shown in Fig. 38. They also identified and compared the dehumidification/regeneration performance in a falling film internal cooling/heating dehumidifier/regenerator with and without the PVP surfactant. The experimental results indicated that the dehumidification/regeneration rate could be enhanced up to 22.7%/26.3%, which was caused by the increased wetting area (shown in Fig. 39) and the decrease in falling-film thickness. In fact, other kinds of surfactants, such as alkyl glucoside [144] and 2-methyl-1-pentanol [145], were also used by previous researchers to improve the absorption performance, and different degrees of enhancement were observed. A summary for some of the experimental studies on heat and mass transfer enhancement by surfactants is specified in Table 10.

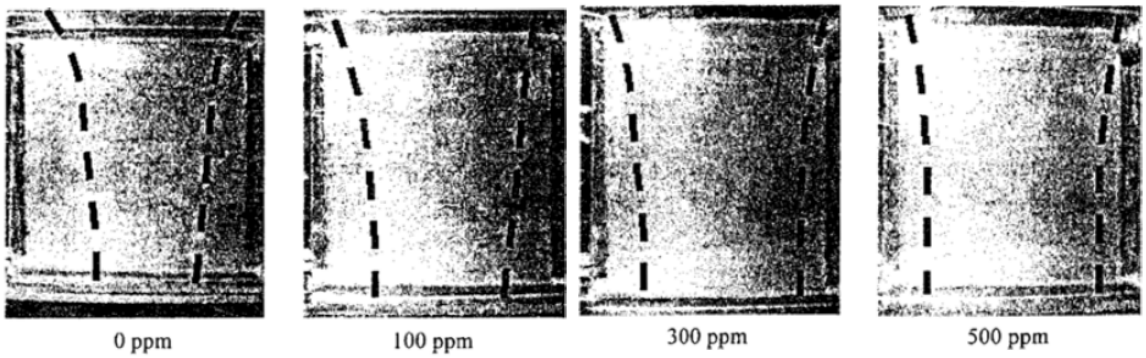

Fig. 37. Effect of surfactant concentration on falling-film flow pattern [142].

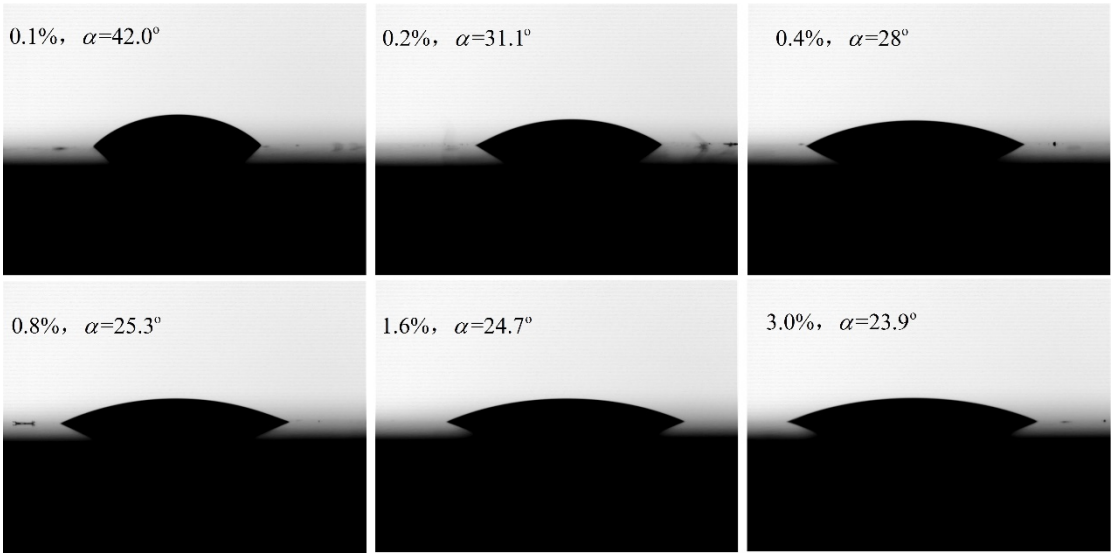

Fig. 38. Contact angles of LiCl solution with different concentrations of PVP [143].

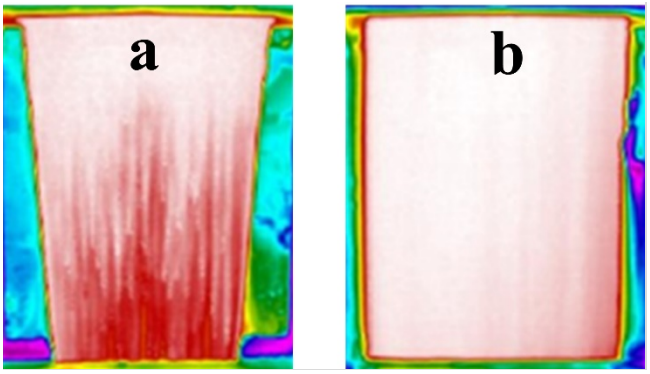

Fig. 39. Contrast of wettability of falling film (a) without surfactant and (b) with PVP surfactant [143].

Table. 10. Comparison between different kinds of surfactants.

Author	Mode[a]	Solution[b]	Surfactant	Toxicity	Odour	Enhancement
Cosenza & Vliet [121]	FA	LiBr/H_2O	2-ethyl-1-hexanol	High	Yes	3~4
Hozawa et al. [140]	SA	LiBr/H_2O	n-octanol n-decanol	Small	Yes	~2.5
Hihara & Saito [136]	FA	LiBr/H_2O	2-ethyl-1-hexanol	High	Yes	4~5
Perez-Blanco & Sheehan [137]	FA	LiBr/H_2O	2-ethyl-1-hexanol	High	Yes	~0.35
Kyung & Herold [146]	FA	LiBr/H_2O	2-ethyl-hexanol	Small	Yes	1.2-1.7
Glebov et al. [145]	FA	LiBr/H_2O	2-methyal-1-pentanol	Small	Yes	0.2-0.32
Rivera & Cerezo [138]	FA	LiBr/H_2O	1-octanol 2-ethyl-1-hexanol	High	Yes	~0.4
Kim et al. [147]	BA	NH_3/H_2O	2-ethyl-1-hexanol, n-octanol	Small	Yes	~ 4.81
Kang et al. [142]	FH	H_2O	Triton X-100	Small	Yes	
Sun & Zhang et al. [139]	FA	LiBr/H_2O	2-ethyl-1-hexanol	High	Yes	1.9-2.5
Wen et al. [143]	De	LiCl/H_2O	Polyvinyl Pyrrolidone	No	No	0.08-0.4

a: FA: falling film absorption; SA: static absorption; BA: bubble absorption; FH: falling-film heat transfer; De: dehumidification;

There are several explanations to interpret the significant improvement of heat and mass transfer performance by adding only a tiny amount of surfactant. Kang et al. [142] and Wen et al. [75, 143] attributed the enhancement to the improvement of wettability and the decrease in the falling-film thickness. In fact, such changes in terms of flow pattern may be caused by the reduction of liquid surface tension after adding the surfactant, which were partly verified by the findings of Daiguji et al. [148] and Kulankara and Herold [149]. Daiguji et al. [148] stated that the surface tension of liquid had a significant effect on the absorption performance, and Kulankara and Herold [149] experimentally found that the addition of surfactants reduced the surface tension up to a critical degree with the increase of surfactant concentration. Other scholars thought that the enhancement was caused by the Marangoni convection, which was caused by the imbalance of surface tension between different phase interfaces, as shown in Fig. 40 [150]. However, the trigger

mechanism for Marangoni convection is still unclear. Some possible theories, such as the Kashiwagi model [151], the salting-out model [148], the solubility model [152] and the vapour surfactant theory [153], have tried to give a reasonable interpretation for the trigger mechanism. However, they can only partly explain the experimental phenomenon; their explanations are not applicable for all experimental observations.

It is worth noting that all studies except for those conducted by Kang et al. [142] and Wen et al. [75, 143], focused on absorption refrigeration. Because the aqueous solution, such as a LiCl or LiBr solution, circulates in a closed loop in an absorption refrigerant system, the volatility and odour of the surfactants do not matter in such system. However, in an open-type LDCS, the aqueous solution comes into direct contact with the air, which will be delivered to the air-conditioned room. The volatility and odour of the surfactant are thus impermissible for the consideration of residents' health. Therefore, looking for a surfactant without volatility and odour has become one of the main challenges in the field of heat and mas transfer enhancement by adding surfactants in LDCSs.

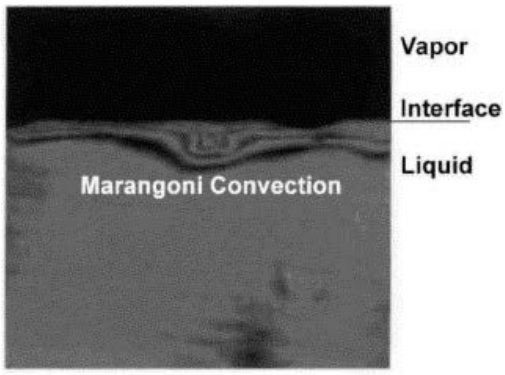

Fig. 40. Photograph of the Marangoni convection [150].

5.2 Addition of nanoparticles

In order to overcome the inherent drawback of poor thermal conductivity of conventional fluids, certain amount of fine particles are dispersed into the basefluid to increase the thermal conductivity and heat and mass transfer performance. The modified fluid with particles is called nanofluid which is defined to be the stable lyosol with ultrafine particles of diameter less than 100nm [154]. In the last few decades, more and more attention has been paid to nanofluid since it was observed with significant enhancement in heat and mass transfer [155, 156].

Kang et al. [157] experimentally investigated the absorption performance of LiCl solution in a falling film tube-type absorber with the adding of carbon nanotubes (CNT) and Fe nanoparticles.

In order to evenly distribute the nanoparticle into LiCl solution, an ultrasonic vibrator and the surfactant of Arabic gum were employed. Their results revealed that the mass transfer enhancement by adding CNT (average 2.16 for 0.01 wt % and average 2.48 for 0.1 wt %) was higher than that of Fe nanoparticles (average 1.71 for 0.01 wt % and average 1.90 for 0.1 wt %). Yang et al. [158] identified the absorption performance of NH_3/H_2O in a falling film tube absorber. Three kinds of nanoparticles, namely $ZnFe_2O_4$, Al_2O_3 and Fe_2O_3, were added into the basefluid of NH_3/H_2O solution. Sodium dodecyl benzene sulfonate was firstly mixed with the three nanoparticles in the NH_3/H_2O basefluid. Then, two hours of mechanical agitation and 30 minutes of ultrasonic vibration were exerted on the mixed solution to get the stable nano-particle suspension of ammonia–water solution. By analysing the experimental results, they found that the absorption performance was weakened by only adding surfactant or adding poorly dispersed nanoparticles. When the nanoparticles were well dispersed into the basefluid, the effective absorption ratio could be increased up to 50% and 70% with the adding of $ZnFe_2O_4$ and Fe_2O_3 nanoparticles at the ammonia mass fraction of 15%. Kim et al. [159] performed similar experimental study with that of Kang et al. [157] but with the adding of SiO_2 nanoparticles. They revealed that the SiO_2 nanoparticles could be evenly and steadily dispersed into $LiBr/H_2O$ solution only when the concentration of SiO_2 was less than 0.01 vol%. Otherwise, surfactant was required for steady dispersion. The absorption rate was increased up to 18% when the SiO_2 concentration was 0.005 vol%, which was caused by Brownian motion. Pineda et al. [160] experimentally identified the CO_2 absorption performance of methanol with the adding of Al_2O_3 and SiO_2 nanoparticles in a tray column absorber. They used an ultra-sonicator for the dispersion of SiO_2 nanoparticles during their preparation of methanol-based nanofluid. The maximum enhancement ratios of 9.4% and 9.7% for Al_2O_3 and SiO_2 were detected during their experiments at the concentration of 0.05 vol%. Zhang et al. [161] dispersed the Fe_3O_4 nanoparticles into LiBr solution to investigate its absorption performance in a falling film absorber. They indicated that the mass transfer enhancement ratio increased with the decrease of particle size. The enhancement ratio could reach up to 2.28 times for the particle size of 20nm and concentration of 0.05 wt%. As one can see, surfactant is often added into the basefluid as a stabilizer. However, except Yang et al. [158] who identified the influence of surfactant alone, other researchers who adopted surfactant all failed to solely investigate the effect of surfactant on mass transfer performance. It is worth noting that the abovementioned literatures are all about absorption refrigeration. Few previous

studies concern the liquid desiccant dehumidification/regeneration and the existing ones are summarized in the following part.

Ali et al. [162, 163] studied the dehumidification performance of $CaCl_2$ in vertical and inclined plate falling film dehumidifiers with the addition of Cu-ultrafine particles by numerical method. The flow patterns between solution and air were parallel flow, counter flow and cross flow. They indicated that the addition of tiny amount of Cu-ultrafine particles had negligible influence on the dehumidification performance. However, they did not conduct any experiments to validate their numerical findings. Wen et al. [164, 165] first dispersed the multi-walled carbon nanotubes (MWNTs) into LiCl solution through mechanical and chemical methods. High speed agitation and ultrasonic vibration along with the addition of surfactant PVP were adopted for the stable dispersion. The dehumidification/regeneration performance of an internal cooling/heating plate-type dehumidifier/regenerator under various operating conditions were experimentally investigated and compared with and without MWNTs. Results showed that the average relative enhancements for dehumidification/regeneration were 25.9%/24.7% for nanofluid. However, they also found that the enhancements could only be attributed to the adding of surfactant PVP. The adding of 0.1 wt% MWNTs into LiCl solution with surfactant shown negligible influence on mass transfer performance. Table 11 summarizes the research on falling film absorption by adding different kinds of nanoparticles.

Table. 11. Comparison between different kinds of nanofluids.

Author	Mode[a]	Basefluid	Nanoparticle	Dispersion method[b]	Method[c]	Enhancement
Kang et al. [157]	FA	$LiCl/H_2O$	CNT, Fe	UV, Arabic gum	E	1.71~2.48
Yang et al. [158]	FA	NH_3/H_2O	$ZnFe_2O_4$, Al_2O_3, Fe_2O_3	MA, UV, SDBS	E	0.5~0.7
Kim et al. [159]	FA	$LiBr/H_2O$	SiO_2		E	~0.18
Pineda et al. [160]	FA	CH_3OH/H_2O	Al_2O_3, SiO_2	UV	E	0.094~0.097
Zhang et al. [161]	FA	$LiBr/H_2O$	Fe_3O_4			~2.28
Ali et al. [162, 163]	De	$CaCl_2/H_2O$	Cu		N	
Wen et al. [164, 165]	De	$LiCl/H_2O$	MWNTs	MA, UV, PVP	E	Average 25%

a: FA: falling film absorption; De: dehumidification;
b: UV: ultrasonic vibration; MA: mechanical agitation;
c: E: experimental study; N: Numerical study;

6 Conclusions

This paper presents an overview of the empirical correlations for performance criteria during dehumidification/regeneration and heat and mass transfer enhancement approaches to improve the efficiency of liquid desiccant cooling systems. The concluding remarks and some suggestions for future work are summarised and outlined as follows.

(1) There are numerous empirical correlations to predict the mass transfer coefficient and moisture effectiveness during dehumidification/regeneration for both adiabatic and internal cooling/heating type dehumidifier/regenerators. Most of these correlations are based on the experimental data obtained by the authors themselves, which results in a lack of general applicability.

(2) The internal cooling/heating type dehumidifier/regenerator is a promising alternative for the conventional adiabatic one owing to its higher efficiency and less possibility of liquid carryover. To further improve its heat and mass transfer performance, it must be designed with a compact structure, such as tube-fin type or plate type. Because these types are very similar to those adopted in the field of single-phase heat exchangers, the efficiency enhancement methods, such as the use of a fin structure for the purpose of flow disturbance and increasing the contact surface, can be applied in the dehumidifier/regenerator for heat and mass transfer enhancement.

(3) Surface modification by chemical and physical methods is an effective way to improve dehumidification/regeneration performance. The use of a hydrophilic coating or fabric on the surface of the dehumidifier/regenerator would not only improve the wettability but also change the flow behaviour on the plate.

(4) Ultrasound can make the liquid desiccant atomise into numerous fine droplets, which significantly increases the contact area between the solution and the air. As a result, the dehumidification/regeneration performance is also enhanced by ultrasound atomisation.

(5) Membrane-based dehumidifier/regenerators can effectively overcome the problem of liquid carryover by totally separating the air and liquid. These membranes also can be constructed with high specific contact areas and internal cooling/heating for higher efficiency.

(6) Adding surfactants to the liquid solution can remarkably increase the absorption rate in an absorption refrigeration system. In view of the similar working principle between absorption refrigeration and liquid desiccant cooling system, the mass transfer performance in a liquid desiccant cooling system is also likely to be enhanced by the addition of certain kinds of surfactants. However, considering the application of a liquid desiccant cooling system in air-conditioned areas,

the surfactant must be non-volatile, odourless and nontoxic, which provides strict requirements in the screening of possible surfactant candidates.

(7) The addition of nanoparticles into a liquid desiccant can improve the mass transfer performance to different degrees. Owing to the special chemical properties of liquid desiccants, achieving stable and even dispersion of nanoparticles in the desiccant is a great challenge.

7 Suggestions for future work

Based on the above conclusive remarks, some recommendations for future work are summarised as follows:

(1) For the convenience of engineering applications, it is meaningful to develop some widely accepted correlations for dehumidifier/regenerators with different configurations and materials based on the existing and self-acquired experimental data. Especially for internal cooling/heating dehumidifier/ regenerators, because their structure is relatively monomorphic, a widely acceptable correlation for mass transfer coefficient based on numerous experiments is proposed. Moreover, it would be helpful and necessary to give detailed information regarding the experimental conditions and the structural parameters of the components.

(2) A considerable issue for metal-based dehumidifier/regenerators is the metal corrosion caused by the use of a liquid desiccant. The corrosion of metals has a great effect on heat and mass transfer performance and system stability. Therefore, future studies must address this problem by finding alternatives for conventional salt-based liquid desiccants and developing anti-corrosion plate technologies.

(3) The adoption of ultrasound atomisation will cause liquid carryover in the system. To fulfil the practical application, the liquid carryover must be overcome and avoided before the large-scale application of ultrasound atomisation.

(4) For the application of membrane-based dehumidifier/regenerators, some problems, such as the poor tolerance of the membrane at high temperature, particulate contamination and crystallisation of the desiccant, must be solved before its wide application.

(5) As a stabiliser in a nanofluid, it is also important to investigate the influence of surfactants on mass transfer alone. Moreover, the enhancement mechanism by adding nanoparticles remains unclear, and thus it must be uncovered in future studies.

Acknowledgement

The work is financially supported by Hong Kong Research Grant Council through General Research Fund (PolyU 152010/15E).

References

[1] Huang Y, Niu J-l, Chung T-m. Energy and carbon emission payback analysis for energy-efficient retrofitting in buildings—Overhang shading option. Energy and Buildings. 2012;44:94-103.
[2] De Dear RJ, Brager GS. Thermal comfort in naturally ventilated buildings: revisions to ASHRAE Standard 55. Energy and buildings. 2002;34:549-61.
[3] Nicol JF, Humphreys MA. Adaptive thermal comfort and sustainable thermal standards for buildings. Energy and buildings. 2002;34:563-72.
[4] Nicol F. Adaptive thermal comfort standards in the hot–humid tropics. Energy and buildings. 2004;36:628-37.
[5] Efficiency E. Buildings energy data book. US Department of Energy. 2009.
[6] China Building Energy Use 2017,https://berc.bestchina.org/Files/CBEU2017.pdf.
[7] Koroneos C, Tsarouhis M. Exergy analysis and life cycle assessment of solar heating and cooling systems in the building environment. Journal of Cleaner Production. 2012;32:52-60.
[8] Fekadu G, Subudhi S. Renewable energy for liquid desiccants air conditioning system: A review. Renewable and Sustainable Energy Reviews. 2018;93:364-79.
[9] IEA. Key world energy statistics. France: International Energy Agency, 2008.
[10] Qi R, Lu L, Yang H. Development of simplified prediction model for internally cooled/heated liquid desiccant dehumidification system. Energy and buildings. 2013;59:133-42.
[11] Ge G, Xiao F, Niu X. Control strategies for a liquid desiccant air-conditioning system. Energy and buildings. 2011;43:1499-507.
[12] Wen T, Zhan H, Zhang D, Lu L. Development of evaporation pressure-capacity control strategy for aircraft vapor cycle system. International Journal of Refrigeration. 2017;83:14-22.
[13] Wen T, Lu L. Numerical and experimental study on internally cooled liquid desiccant dehumidification concerning film shrinkage shape and vapor condensation. International Journal of Thermal Sciences. 2019;136:316-27.
[14] She X, Cong L, Nie B, Leng G, Peng H, Chen Y, et al. Energy-efficient and-economic technologies for air conditioning with vapor compression refrigeration: A comprehensive review. Applied Energy. 2018;232:157-86.
[15] Luo Y, Yang H, Lu L. Dynamic and microscopic simulation of the counter-current flow in a liquid desiccant dehumidifier. Applied Energy. 2014;136:1018-25.
[16] Luo Y, Wang M, Yang H, Lu L, Peng J. Experimental study of internally cooled liquid desiccant dehumidification: application in Hong Kong and intensive analysis of influencing factors. Building and Environment. 2015;93:210-20.
[17] Grossman G, Johannsen A. Solar cooling and air conditioning. Progress in Energy and Combustion Science. 1981;7:185-228.
[18] Zhang L-Z, Zelik EB. Total heat recovery: heat and moisture recovery from ventilation air: Nova Science Publ.; 2008.
[19] Ou X, Cai W, He X, Zhai D. Experimental investigations on heat and mass transfer performances of a liquid desiccant cooling and dehumidification system. Applied Energy. 2018;220:164-75.
[20] Luo Y, Chen Y, Yang H, Wang Y. Study on an internally-cooled liquid desiccant dehumidifier with CFD model. Applied energy. 2017;194:399-409.

[21] Wan KK, Li DH, Liu D, Lam JC. Future trends of building heating and cooling loads and energy consumption in different climates. Building and Environment. 2011;46:223-34.
[22] Conde MR. Properties of aqueous solutions of lithium and calcium chlorides: formulations for use in air conditioning equipment design. International Journal of Thermal Sciences. 2004;43:367-82.
[23] Patek J, Klomfar J. A computationally effective formulation of the thermodynamic properties of LiBr–H2O solutions from 273 to 500 K over full composition range. International Journal of Refrigeration. 2006;29:566-78.
[24] Kaita Y. Thermodynamic properties of lithium bromide–water solutions at high temperatures. International Journal of refrigeration. 2001;24:374-90.
[25] Luo Y, Shao S, Xu H, Tian C, Yang H. Experimental and theoretical research of a fin-tube type internally-cooled liquid desiccant dehumidifier. Applied Energy. 2014;133:127-34.
[26] Wen T, Lu L, Yang H, Luo Y. Investigation on the Regeneration and Corrosion Characteristics of an Anodized Aluminum Plate Regenerator. Energies. 2018;11:1-15.
[27] Wen T, Lu L, Dong C, Luo Y. Development and experimental study of a novel plate dehumidifier made of anodized aluminum. Energy. 2018;144:169-77.
[28] Islam M, Alan S, Chua K. Studying the heat and mass transfer process of liquid desiccant for dehumidification and cooling. Applied Energy. 2018;221:334-47.
[29] Qi R, Lu L. Energy consumption and optimization of internally cooled/heated liquid desiccant air-conditioning system: A case study in Hong Kong. Energy. 2014;73:801-8.
[30] Qi R, Lu L, Huang Y. Parameter analysis and optimization of the energy and economic performance of solar-assisted liquid desiccant cooling system under different climate conditions. Energy Conversion and Management. 2015;106:1387-95.
[31] Zhang N, Yin S-Y, Li M. Model-based optimization for a heat pump driven and hollow fiber membrane hybrid two-stage liquid desiccant air dehumidification system. Applied Energy. 2018;228:12-20.
[32] Shan N, Yin Y, Zhang X. Study on performance of a novel energy-efficient heat pump system using liquid desiccant. Applied Energy. 2018;219:325-37.
[33] Daou K, Wang R, Xia Z. Desiccant cooling air conditioning: a review. Renewable and Sustainable Energy Reviews. 2006;10:55-77.
[34] Mei L, Dai Y. A technical review on use of liquid-desiccant dehumidification for air-conditioning application. Renewable and Sustainable Energy Reviews. 2008;12:662-89.
[35] Cheng Q, Zhang X. Review of solar regeneration methods for liquid desiccant air-conditioning system. Energy and Buildings. 2013;67:426-33.
[36] Mohammad AT, Mat SB, Sulaiman MY, Sopian K, Al-Abidi AA. Historical review of liquid desiccant evaporation cooling technology. Energy and Buildings. 2013;67:22-33.
[37] Yin Y, Qian J, Zhang X. Recent advancements in liquid desiccant dehumidification technology. Renewable and Sustainable Energy Reviews. 2014;31:38-52.
[38] Luo Y, Yang H, Lu L, Qi R. A review of the mathematical models for predicting the heat and mass transfer process in the liquid desiccant dehumidifier. Renewable and Sustainable Energy Reviews. 2014;31:587-99.
[39] Buker MS, Riffat SB. Recent developments in solar assisted liquid desiccant evaporative cooling technology—A review. Energy and Buildings. 2015;96:95-108.
[40] Rafique MM, Gandhidasan P, Bahaidarah HM. Liquid desiccant materials and dehumidifiers–A review. Renewable and Sustainable Energy Reviews. 2016;56:179-95.
[41] Abdel-Salam AH, Simonson CJ. State-of-the-art in liquid desiccant air conditioning equipment and systems. Renewable and Sustainable Energy Reviews. 2016;58:1152-83.
[42] Gómez-Castro FM, Schneider D, Päßler T, Eicker U. Review of indirect and direct solar thermal regeneration for liquid desiccant systems. Renewable and Sustainable Energy Reviews. 2018;82:545-75.

[43] Kumar R, Dhar P, Jain S. Development of new wire mesh packings for improving the performance of zero carryover spray tower. Energy. 2011;36:1362-74.
[44] Bravo JL, Rocha J, Fair J. Pressure drop in structured packings. Hydrocarbon Process;(United States). 1986;65.
[45] Chung T-W, Ghosh TK, Hines AL. Comparison between random and structured packings for dehumidification of air by lithium chloride solutions in a packed column and their heat and mass transfer correlations. Industrial & engineering chemistry research. 1996;35:192-8.
[46] Saman WY, Alizadeh S. An experimental study of a cross-flow type plate heat exchanger for dehumidification/cooling. Solar Energy. 2002;73:59-71.
[47] Liu X, Chang X, Xia J, Jiang Y. Performance analysis on the internally cooled dehumidifier using liquid desiccant. Building and Environment. 2009;44:299-308.
[48] Wen T, Wang M, Chen Y, He W, Luo Y. Thermal properties study and performance investigation of potassium formate solution in a falling film dehumidifier/regenerator. International Journal of Heat and Mass Transfer. 2019;134:131-42.
[49] Wen T, Luo Y, He W, Gang W, Sheng L. Development of a novel quasi-3D model to investigate the performance of a falling film dehumidifier with CFD technology. International Journal of Heat and Mass Transfer. 2019;132:431-42.
[50] Yang Z, Lian Z, Li X, Zhang K. Concept of dehumidification perfectness and its potential applications. Energy. 2015;91:176-91.
[51] Onda K, Takeuchi H, Okumoto Y. Mass transfer coefficients between gas and liquid phases in packed columns. Journal of chemical engineering of Japan. 1968;1:56-62.
[52] Babakhani D, Soleymani M. Simplified analysis of heat and mass transfer model in liquid desiccant regeneration process. Journal of the Taiwan Institute of Chemical Engineers. 2010;41:259-67.
[53] Babakhani D, Soleymani M. An analytical solution for air dehumidification by liquid desiccant in a packed column. International Communications in Heat and Mass Transfer. 2009;36:969-77.
[54] Jain S, Bansal P. Performance analysis of liquid desiccant dehumidification systems. International Journal of Refrigeration. 2007;30:861-72.
[55] Fumo N, Goswami D. Study of an aqueous lithium chloride desiccant system: air dehumidification and desiccant regeneration. Solar energy. 2002;72:351-61.
[56] Chung T-W, Ghosh TK, Hines AL, Novosel D. Dehumidification of moist air with simultaneous removal of selected indoor pollutants by triethylene glycol solutions in a packed-bed absorber. Separation Science and Technology. 1995;30:1807-32.
[57] Chung T-W, Ghosh TK, Hines AL. Dehumidification of air by aqueous lithium chloride in a packed column. Separation Science and Technology. 1993;28:533-50.
[58] Koronaki I, Christodoulaki R, Papaefthimiou V, Rogdakis E. Thermodynamic analysis of a counter flow adiabatic dehumidifier with different liquid desiccant materials. Applied Thermal Engineering. 2013;50:361-73.
[59] Hong kong Energy End-use Data 2015, https://www.emsd.gov.hk/filemanager/en/content_762/HKEEUD2015.pdf.
[60] Elsarrag E, Magzoub EE, Jain S. Mass-transfer correlations for dehumidification of air by triethylene glycol in a structured packed column. Industrial & engineering chemistry research. 2004;43:7676-81.
[61] Liu X, Jiang Y, Qu K. Heat and mass transfer model of cross flow liquid desiccant air dehumidifier/regenerator. Energy Conversion and Management. 2007;48:546-54.
[62] Chung T-W, Wu H. Comparison between spray towers with and without fin coils for air dehumidification using triethylene glycol solutions and development of the mass-transfer correlations. Industrial & engineering chemistry research. 2000;39:2076-84.

[63] Zhang L, Hihara E, Matsuoka F, Dang C. Experimental analysis of mass transfer in adiabatic structured packing dehumidifier/regenerator with liquid desiccant. International Journal of Heat and Mass Transfer. 2010;53:2856-63.
[64] Langroudi LO, Pahlavanzadeh H, Mousavi S. Statistical evaluation of a liquid desiccant dehumidification system using RSM and theoretical study based on the effectiveness NTU model. Journal of Industrial and Engineering Chemistry. 2014;20:2975-83.
[65] Su W, Li W, Sun B, Zhang X. Experimental study and correlations for heat and mass transfer coefficients in the dehumidifier of a frost-free heat pump system. International Journal of Heat and Mass Transfer. 2019;131:450-62.
[66] Varela RJ, Yamaguchi S, Giannetti N, Saito K, Harada M, Miyauchi H. General correlations for the heat and mass transfer coefficients in an air-solution contactor of a liquid desiccant system and an experimental case application. International Journal of Heat and Mass Transfer. 2018;120:851-60.
[67] Bassuoni M. An experimental study of structured packing dehumidifier/regenerator operating with liquid desiccant. Energy. 2011;36:2628-38.
[68] Chen T, Dai Z, Yin Y, Zhang X. Experimental investigation on the mass transfer performance of a novel packing used for liquid desiccant systems. Science and Technology for the Built Environment. 2017;23:46-59.
[69] Huang S, Lv Z, Zhang X, Liang C. Experimental investigation on heat and mass transfer in heating tower solution regeneration using packing tower. Energy and Buildings. 2018;164:77-86.
[70] Yin Y, Zhang X, Peng D, Li X. Model validation and case study on internally cooled/heated dehumidifier/regenerator of liquid desiccant systems. International journal of thermal sciences. 2009;48:1664-71.
[71] Qi R. Study on heat and mass transfer of internally heated liquid desiccant regeneration for solar-assisted air-conditioning system: The Hong Kong Polytechnic University; 2013.
[72] Liu J, Zhang T, Liu X, Jiang J. Experimental analysis of an internally-cooled/heated liquid desiccant dehumidifier/regenerator made of thermally conductive plastic. Energy and Buildings. 2015;99:75-86.
[73] Lee JH, Jung CW, Chang YS, Chung JT, Kang YT. Nu and Sh correlations for LiCl solution and moist air in plate type dehumidifier. International Journal of Heat and Mass Transfer. 2016;100:433-44.
[74] Dong C, Lu L, Wen T. Experimental study on dehumidification performance enhancement by TiO2 superhydrophilic coating for liquid desiccant plate dehumidifiers. Building and Environment. 2017;124:219-31.
[75] Wen T, Lu L, Dong C, Luo Y. Investigation on the regeneration performance of liquid desiccant by adding surfactant PVP-K30. International Journal of Heat and Mass Transfer. 2018;123:445-54.
[76] Jain S, Dhar P, Kaushik S. Experimental studies on the dehumidifier and regenerator of a liquid desiccant cooling system. Applied thermal engineering. 2000;20:253-67.
[77] Hassan MS, Hassan A. Performance of a proposed complete wetting surface counter flow channel type liquid desiccant air dehumidifier. Renewable Energy. 2009;34:2107-16.
[78] Mesquita L, Harrison S, Thomey D. Modeling of heat and mass transfer in parallel plate liquid-desiccant dehumidifiers. Solar Energy. 2006;80:1475-82.
[79] Chung T-W. Predictions of moisture removal efficiencies for packed-bed dehumidification systems. Gas separation & purification. 1994;8:265-8.
[80] Martin V, Goswami DY. Effectiveness of heat and mass transfer processes in a packed bed liquid desiccant dehumidifier/regenerator. Hvac&R Research. 2000;6:21-39.
[81] Martin V, Goswami D. Heat and mass transfer in packed bed liquid desiccant regenerators-an experimental investigation. Journal of Solar Energy Engineering-Transactions of The ASME. 1999;121:162-70.
[82] Oberg V, Goswami DY. Experimental study of the heat and mass transfer in a packed bed liquid desiccant air dehumidifier. Journal of Solar Energy Engineering. 1998;120:289-97.

[83] Oberg V. Heat and mass transfer study of a packed bed absorber/regenerator for solar desiccant cooling. PhD thesis, University of Florida ,1999.
[84] Abdul-Wahab S, Zurigat Y, Abu-Arabi M. Predictions of moisture removal rate and dehumidification effectiveness for structured liquid desiccant air dehumidifier. Energy. 2004;29:19-34.
[85] Liu X, Qu K, Jiang Y. Empirical correlations to predict the performance of the dehumidifier using liquid desiccant in heat and mass transfer. Renewable Energy. 2006;31:1627-39.
[86] Liu X, Zhang Y, Qu K, Jiang Y. Experimental study on mass transfer performances of cross flow dehumidifier using liquid desiccant. Energy Conversion and Management. 2006;47:2682-92.
[87] Moon C, Bansal P, Jain S. New mass transfer performance data of a cross-flow liquid desiccant dehumidification system. International journal of refrigeration. 2009;32:524-33.
[88] Gao W, Liu J, Cheng Y, Zhang X. Experimental investigation on the heat and mass transfer between air and liquid desiccant in a cross-flow dehumidifier. Renewable Energy. 2012;37:117-23.
[89] Wang L, Xiao F, Zhang X, Kumar R. An experimental study on the dehumidification performance of a counter flow liquid desiccant dehumidifier. International Journal of Refrigeration. 2016;70:289-301.
[90] Chen Y, Yin Y, Zhang X. Performance analysis of a hybrid air-conditioning system dehumidified by liquid desiccant with low temperature and low concentration. Energy and Buildings. 2014;77:91-102.
[91] Yin Y, Zhang X, Wang G, Luo L. Experimental study on a new internally cooled/heated dehumidifier/regenerator of liquid desiccant systems. International Journal of Refrigeration. 2008;31:857-66.
[92] Khan AY. Cooling and dehumidification performance analysis of internally-cooled liquid desiccant absorbers. Applied Thermal Engineering. 1998;18:265-81.
[93] Zhang T, Liu X, Jiang J, Chang X, Jiang Y. Experimental analysis of an internally-cooled liquid desiccant dehumidifier. Building and environment. 2013;63:1-10.
[94] Wen T, Lu L, Nie Y, Zhong H. Development and investigation on the dehumidification and corrosion resistance performance of a new mixed liquid desiccant. International Journal of Heat and Mass Transfer. 2019;130:72-82.
[95] Wen T, Lu L, Li M, Zhong H. Comparative study of the regeneration characteristics of LiCl and a new mixed liquid desiccant solution. Energy. 2018.
[96] Isshiki N, Ogawa K. Enhancement of heat and mass transfer by CCS tubes. PrOCeedingS Of the Intermational Ab-SOrption Heat Pump Conference, Montreal, Camada, VOl1996. p. 335-41.2.
[97] Yoon J-I, Kwon O-K, Moon C-G. Experimental investigation of heat and mass transfer in absorber with enhanced tubes. KSME International Journal. 1999;13:640-6.
[98] Park CW, Kim SS, Cho HC, Kang YT. Experimental correlation of falling film absorption heat transfer on micro-scale hatched tubes. International journal of refrigeration. 2003;26:758-63.
[99] Isshiki N, Ogawa K. Enhancement of heat and mass transfer by CCS tubes, Ab-Sorption 96. Proceedings of the ISHPC, Montreal, Canada[Links]. 1996.
[100] Islam MR, Wijeysundera N, Ho J. Performance study of a falling-film absorber with a film-inverting configuration. International Journal of Refrigeration. 2003;26:909-17.
[101] Cui X-Y, Shi J-Z, Tan C, Xu Z-P. Investigation of plate falling film absorber with film-inverting configuration. Journal of Heat Transfer. 2009;131:072001.
[102] Mortazavi M, Isfahani RN, Bigham S, Moghaddam S. Absorption characteristics of falling film LiBr (lithium bromide) solution over a finned structure. Energy. 2015;87:270-8.
[103] Ren CQ, Tu M, Wang HH. An analytical model for heat and mass transfer processes in internally cooled or heated liquid desiccant–air contact units. International Journal of Heat and Mass Transfer. 2007;50:3545-55.
[104] Peng C, Howell JR. The performance of various types of regenerators for liquid desiccants. J Sol Energy Eng;(United States). 1984;106.

[105] Wang Q, Ma X, Lan Z, Chen J, Bai T. Heat transfer characteristics of falling film process on coated division tubes: effect of the surface configurations. Industrial & Engineering Chemistry Research. 2010;49:6622-9.
[106] Qi R, Hu Y, Wang Y, Lu L. A new approach to enhance the heat and mass transfer of liquid desiccant dehumidification with a titanium dioxide superhydrophilic self-cleaning coating. Journal of Cleaner Production. 2016;112:3555-61.
[107] Dong C, Lu L, Qi R. Model development of heat/mass transfer for internally cooled dehumidifier concerning liquid film shrinkage shape and contact angles. Building and Environment. 2017;114:11-22.
[108] Lun W, Li K, Liu B, Zhang H, Yang Y, Yang C. Experimental analysis of a novel internally-cooled dehumidifier with self-cooled liquid desiccant. Building and Environment. 2018.
[109] Yao Y. Using power ultrasound for the regeneration of dehumidizers in desiccant air-conditioning systems: A review of prospective studies and unexplored issues. Renewable and sustainable energy reviews. 2010;14:1860-73.
[110] Yasuda K, Bando Y, Yamaguchi S, Nakamura M, Oda A, Kawase Y. Analysis of concentration characteristics in ultrasonic atomization by droplet diameter distribution. Ultrasonics sonochemistry. 2005;12:37-41.
[111] Clift R, Grace JR, Weber ME. Bubbles, drops, and particles: Courier Corporation; 2005.
[112] Yao Y, Yang K, Guo H. Regeneration of liquid desiccant assisted by ultrasonic atomizing. Cryogenics and refrigeration proceedings of ICCR2013, Hangzhou, China. 2013:6-8.
[113] Yang Z, Zhang K, Hwang Y, Lian Z. Performance investigation on the ultrasonic atomization liquid desiccant regeneration system. Applied energy. 2016;171:12-25.
[114] Yao Y, Liu S. Ultrasonic Technology for Desiccant Regeneration: John Wiley & Sons; 2014.
[115] WANG L, LIAN Z-w, LIU W-w. Analysis of liquid-desiccant dehumidifying system combined with ultrasound atomization technology [J]. Journal of Central South University (Science and Technology). 2011;1:040.
[116] Wang L, Lian Z-W. Improvement of conventional liquid desiccant dehumidification technology. Journal of Southeast University (English Edition). 2010;26:212-6.
[117] Yang Z, Zhang K, Yang M, Lian Z. Improvement of the ultrasonic atomization liquid desiccant dehumidification system. Energy and Buildings. 2014;85:145-54.
[118] Bergero S, Chiari A. Experimental and theoretical analysis of air humidification/dehumidification processes using hydrophobic capillary contactors. Applied Thermal Engineering. 2001;21:1119-35.
[119] Isetti C, Nannei E, Magrini A. On the application of a membrane air—liquid contactor for air dehumidification. Energy and Buildings. 1997;25:185-93.
[120] Scovazzo P, Burgos J, Hoehn A, Todd P. Hydrophilic membrane-based humidity control. Journal of membrane science. 1998;149:69-81.
[121] Bai H, Zhu J, Chen Z, Chu J. State-of-art in modelling methods of membrane-based liquid desiccant heat and mass exchanger: a comprehensive review. International Journal of Heat and Mass Transfer. 2018;125:445-70.
[122] Huang S-M, Zhang L-Z. Researches and trends in membrane-based liquid desiccant air dehumidification. Renewable and Sustainable Energy Reviews. 2013;28:425-40.
[123] Yang B, Yuan W, Gao F, Guo B. A review of membrane-based air dehumidification. Indoor and Built Environment. 2015;24:11-26.
[124] Zhang L-Z, Liang C-H, Pei L-X. Heat and moisture transfer in application scale parallel-plates enthalpy exchangers with novel membrane materials. Journal of Membrane Science. 2008;325:672-82.
[125] Defraeye T, Blocken B, Carmeliet J. Analysis of convective heat and mass transfer coefficients for convective drying of a porous flat plate by conjugate modelling. International Journal of Heat and Mass Transfer. 2012;55:112-24.

[126] Zhang L-Z. An analytical solution for heat mass transfer in a hollow fiber membrane based air-to-air heat mass exchanger. Journal of Membrane Science. 2010;360:217-25.
[127] Liu S, Riffat S, Zhao X, Yuan Y. Impact of adsorbent finishing and absorbent filming on energy exchange efficiency of an air-to-air cellulose fibre heat & mass exchanger. Building and Environment. 2009;44:1803-9.
[128] Huang S-M, Zhang L-Z, Tang K, Pei L-X. Fluid flow and heat mass transfer in membrane parallel-plates channels used for liquid desiccant air dehumidification. International journal of heat and mass transfer. 2012;55:2571-80.
[129] Bergman TL, Incropera FP, Lavine AS, Dewitt DP. Introduction to heat transfer: John Wiley & Sons; 2011.
[130] Vali A, Simonson CJ, Besant RW, Mahmood G. Numerical model and effectiveness correlations for a run-around heat recovery system with combined counter and cross flow exchangers. International Journal of Heat and Mass Transfer. 2009;52:5827-40.
[131] Zhang L-Z, Huang S-M, Pei L-X. Conjugate heat and mass transfer in a cross-flow hollow fiber membrane contactor for liquid desiccant air dehumidification. International journal of heat and mass transfer. 2012;55:8061-72.
[132] Huang S-M, Yang M, Hu B, Tao S, Qin FG, Weng W, et al. Performance analysis of an internally-cooled plate membrane liquid desiccant dehumidifier (IMLDD): An analytical solution approach. International Journal of Heat and Mass Transfer. 2018;119:577-85.
[133] Woods J, Kozubal E. On the importance of the heat and mass transfer resistances in internally-cooled liquid desiccant dehumidifiers and regenerators. International Journal of Heat and Mass Transfer. 2018;122:324-40.
[134] Beutler A, Greiter I, Wagner A, Hoffman L, Schreier S, Alefeld G. Surfactants and fluid properties. International journal of refrigeration. 1996;19:342-6.
[135] Cosenza F, Vliet G. Absorption in falling water/LiBr films on horizontal tubes. ASHRAE Trans. 1990;96:693-701.
[136] Hihara E, Saito T. Effect of surfactant on falling film absorption. International journal of refrigeration. 1993;16:339-46.
[137] Perez-Blanco H, Sheehan DS. Effect of additive concentration on falling film absorption. HVAC&R Research. 1995;1:273-81.
[138] Rivera W, Cerezo J. Experimental study of the use of additives in the performance of a single-stage heat transformer operating with water–lithium bromide. International journal of energy research. 2005;29:121-30.
[139] Lin SJF, Shigang Z. Experimental study on vertical vapor absorption into LiBr solution with and without additive. Applied Thermal Engineering. 2011;31:2850-4.
[140] Hozawa M, Inoue M, Sato J, Tsukada T, Imaishi N. Marangoni convection during steam absorption into aqueous LiBr solution with surfactant. Journal of chemical engineering of Japan. 1991;24:209-14.
[141] Ziegler F, Grossman G. Heat-transfer enhancement by additives. International Journal of Refrigeration. 1996;19:301-9.
[142] Kang B, Kim K, Lee D. Fluid flow and heat transfer on a falling liquid film with surfactant from a heated vertical surface. Journal of mechanical science and technology. 2007;21:1807-12.
[143] Wen T, Lu L, Dong C. Enhancing the dehumidification performance of LiCl solution with surfactant PVP-K30. Energy and Buildings. 2018;171:183-95.
[144] Rozenblit R, Gurevich M, Lengel Y, Hetsroni G. Flow patterns and heat transfer in vertical upward air–water flow with surfactant. International Journal of Multiphase Flow. 2006;32:889-901.
[145] Glebov D, Setterwall F. Experimental study of heat transfer additive influence on the absorption chiller performance. International journal of refrigeration. 2002;25:538-45.

[146] Kyung I-S, Herold KE. Performance of horizontal smooth tube absorber with and without 2-ethyl-hexanol. Journal of heat transfer. 2002;124:177-83.
[147] Kim J-K, Jung JY, Kim JH, Kim M-G, Kashiwagi T, Kang YT. The effect of chemical surfactants on the absorption performance during NH 3/H 2 O bubble absorption process. International journal of refrigeration. 2006;29:170-7.
[148] Daiguji H, Hihara E, Saito T. Mechanism of absorption enhancement by surfactant. International journal of heat and mass transfer. 1997;40:1743-52.
[149] Kulankara S, Herold K. Surface tension of aqueous lithium bromide with heat/mass transfer enhancement additives: the effect of additive vapor transport. International journal of refrigeration. 2002;25:383-9.
[150] Kang YT, Kashiwagi T. Heat transfer enhancement by Marangoni convection in the NH 3–H 2 O absorption process. International Journal of Refrigeration. 2002;25:780-8.
[151] Kashiwagi T. Basic mechanism of absorption heat and mass transfer enhancement by the Marangoni effect. Newsletter, IEA Heat Pump Center. 1988;6:2-6.
[152] Kang Y, Akisawa A, Kashiwagi T. Experimental investigation of Marangoni convection in aqueous LiBr solution with additives. Journal of heat transfer. 1999;121.
[153] Kulankara S, Herold KE. Theory of heat/mass transfer additives in absorption chillers. HVAC&R Research. 2000;6:369-80.
[154] Chol S. Enhancing thermal conductivity of fluids with nanoparticles. ASME-Publications-Fed. 1995;231:99-106.
[155] Pang C, Lee JW, Kang YT. Review on combined heat and mass transfer characteristics in nanofluids. International Journal of Thermal Sciences. 2015;87:49-67.
[156] Ashrafmansouri S-S, Esfahany MN. Mass transfer in nanofluids: A review. International Journal of Thermal Sciences. 2014;82:84-99.
[157] Kang YT, Kim HJ, Lee KI. Heat and mass transfer enhancement of binary nanofluids for H 2 O/LiBr falling film absorption process. International Journal of Refrigeration. 2008;31:850-6.
[158] Yang L, Du K, Niu XF, Cheng B, Jiang YF. Experimental study on enhancement of ammonia–water falling film absorption by adding nano-particles. International journal of refrigeration. 2011;34:640-7.
[159] Kim H, Jeong J, Kang YT. Heat and mass transfer enhancement for falling film absorption process by SiO 2 binary nanofluids. International Journal of Refrigeration. 2012;35:645-51.
[160] Pineda IT, Lee JW, Jung I, Kang YT. CO 2 absorption enhancement by methanol-based Al 2 O 3 and SiO 2 nanofluids in a tray column absorber. International journal of refrigeration. 2012;35:1402-9.
[161] Zhang L, Liu Y, Wang Y, Li H, Yang X, Jin L. Experimental Study on Enhanced Falling Film Absorption Process Using H2O/LiBr Nanofluids. ASME 2016 5th International Conference on Micro/Nanoscale Heat and Mass Transfer: American Society of Mechanical Engineers; 2016. p. V001T02A12-VT02A12.
[162] Ali A, Vafai K, Khaled A-R. Analysis of heat and mass transfer between air and falling film in a cross flow configuration. International Journal of Heat and Mass Transfer. 2004;47:743-55.
[163] Ali A, Vafai K. An investigation of heat and mass transfer between air and desiccant film in an inclined parallel and counter flow channels. International Journal of Heat and Mass Transfer. 2004;47:1745-60.
[164] Wen T, Lu L, Zhong H. Investigation on the dehumidification performance of LiCl/H2O-MWNTs nanofluid in a falling film dehumidifier. Building and Environment. 2018;139:8-16.
[165] Wen T, Lu L, Zhong H, Dong C. Experimental and numerical study on the regeneration performance of LiCl solution with surfactant and nanoparticles. International Journal of Heat and Mass Transfer. 2018;127:154-64.